We are IntechOpen,
the world's leading publisher of
Open Access books
Built by scientists, for scientists

6,900
Open access books available

186,000
International authors and editors

200M
Downloads

Our authors are among the

154
Countries delivered to

TOP 1%
most cited scientists

12.2%
Contributors from top 500 universities

CLARIVATE ANALYTICS
BOOK CITATION INDEX
INDEXED

WEB OF SCIENCE™

Selection of our books indexed in the Book Citation Index
in Web of Science™ Core Collection (BKCI)

Interested in publishing with us?
Contact book.department@intechopen.com

Numbers displayed above are based on latest data collected.
For more information visit www.intechopen.com

The Plant Nutrition from the Gas Medium in Greenhouses: Multilevel Simulation and Experimental Investigation

A.V. Vakhrushev, A.Yu. Fedotov, A.A. Vakhrushev,
V.B. Golubchikov and E.V. Golubchikov

Additional information is available at the end of the chapter

http://dx.doi.org/10.5772/53604

1. Introduction

It is extremely important to reduce the action of man-made factors on the environment and vegetables and crops grown in greenhouses. On the one hand, the whole year round, greenhouse technologies provide the production of vegetables and other crops, which contain micro- and macroelements necessary for the vital activity of human being. On the other hand, the use of the technologies implies the use of mineral fertilizers for extra root and foliar nutrition in order to intensify the production. However, despite the use of drop irrigation and small doses of mineral feeding, the concentrations of various heavy metal compounds, radioactive and poisonous substances in the soil of greenhouses reach the limit values after 2–3 years of its service. Then the exhausted soil should be disposed and replaced by new soil, and this is hundreds and thousands of tons.

At the same time, the problem of the neutralization of the used soil arises, since it cannot simply be stored in the open air due to the formation of the dust fractions of the above compounds. In the rain and during snow melting, water-soluble substances penetrate into soil and water sources together with run-off water. From the aforesaid it follows that searching new ways for the nutrition of plants, which allow reducing soil contamination, is urgent. In this regard, the technologies for plant nutrition from the gas phase are quite promising, since the plants receive significant portion of nutrients (up to 80%) through their foliage and stems. It should be noted that controlled gas media have already been used for quite a long time for storing vegetables and fruit. The method is based on the formation of special concentrations of nitrogen, oxygen, carbon dioxide and water vapours in order to reduce the intensity of respiration and metabolism.

Join Stocks Company Nord, (Perm, Russia) has developed a new nanobiotechnology involving nanoparticles for the production of ecologically pure vegetables in greenhouses.

The main feature of the method is the generation of a special controlled gas medium containing nanoparticles of the main macro- and microelements, which freely penetrate into the foliage and stems of crops providing their metabolic activity. The source of the gas medium is the products of self-spreading high-temperature synthesis [1–5].
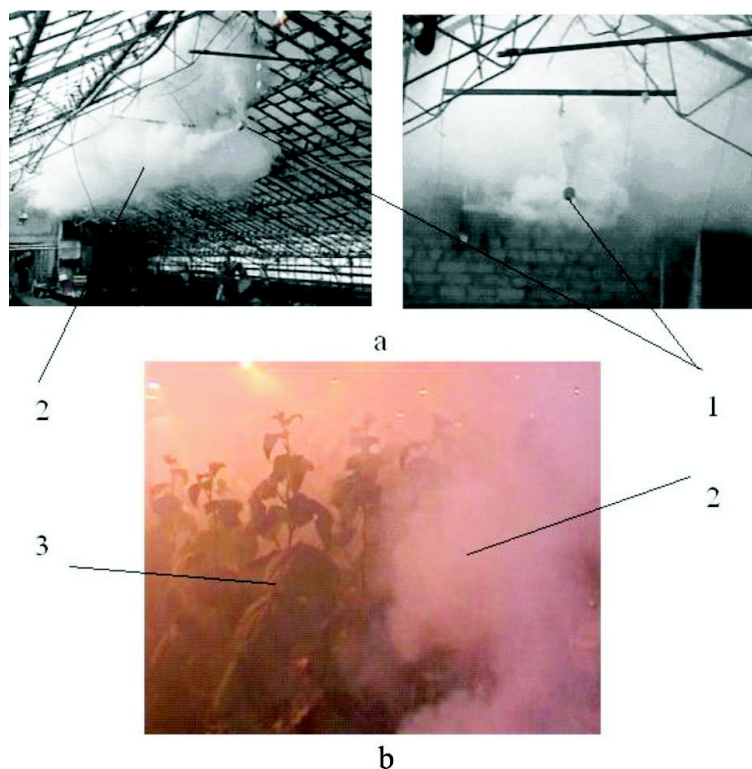

Figure 1. The diagram of the use of gas-generator (1): a) the general view of an industrial greenhouse; b) nanoaerosol gas medium (2) surrounding greenhouse plants (3).

Figure 1 demonstrates the use of a large-size gas-generator for the special controlled gas media (CGM) formation in an industrial greenhouse. CGM is complex media with specially selected concentrations of inorganic compounds in the form of nanoparticles for protecting living systems. They are used for the foliar nutrition of plants with macro- and microelements, the control of living system diseases, the protection of plants against frosts, the seed treatment, etc. The method comprises the creation of a controlled gas medium containing nanoparticles (Figure 2) which can easily penetrate into foliage and stems of plants providing their metabolic activity. The results of the application of the above technology show the absence of carcinogens, heavy metals and other dangerous substances both in foliage and fruits.

The use of this technology for growing various vegetables and crops in greenhouses of Russia, Byelorussia, the Ukraine, China and another countries shows that the controlled gas medium positively influences the metabolism of crops. It increases their productivity, improves their taste properties, reduces the content of harmful substances in them (for example, the content of nitrates is reduced by a factor of ten) and extends the vegetation period, etc. In addition, the use of such a technology cuts the amount of mineral fertilizers applied for the root systems in half. The experimental investigations show that the concentrations of useful substances in a crop leaf increase in two or more times after two-hour exposure to the "nutrient" gas medium.

It should be noted that the high efficiency of the technology of the plant nutrition from the gas medium determines a pressing need to establish certain theoretical aspects and kinetics of the processes taking place when a plant interacts with the substances of the gas medium. It is also necessary to establish the mechanisms of the nanoparticle formation and the evolution regularities for the dynamic interaction processes of condensed nanosystems and plants. In this connection, the experimental investigations and mathematical modeling of the above processes is rather urgent since it allows efficient and many-sided studying the behavior of nanosystems. The analyses of these problems were the purposes of this investigation. Research of processes of occurrence and movement of nanoparticles, being a base element of technology is especially important.
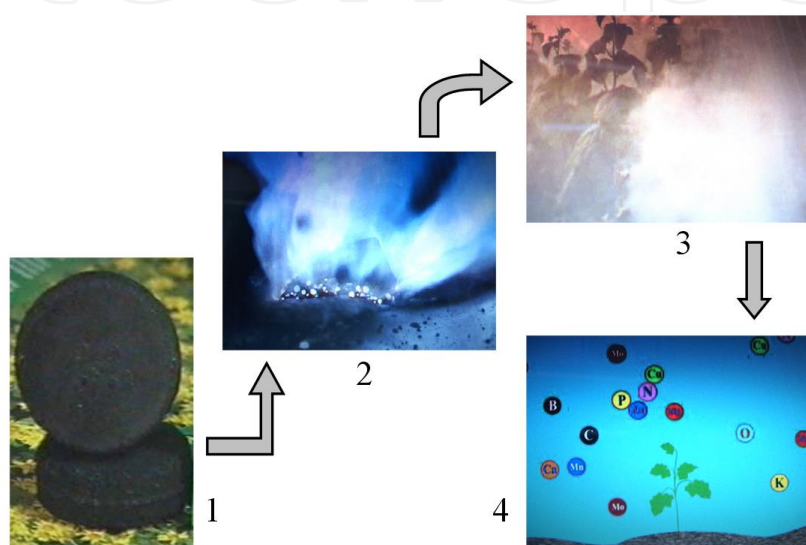
Figure 2. Main steps of biological processes of plant nutrition from controlled gas medium containing nanoparticles: 1 – generation sources, 2 – burning generation sources, 3 – the gas mixture movement from its generation source over the space where the plants are 4 – plant nutrition from gas medium.

2. The task definition. Theoretical base of multilevel simulation and experimental investigations

There are 8 main stages of the processes of the plant nutrition from the gas medium, which follow each other in time (Figure 3):

1. Combustion of a highly condensed system and gas mixture motion from a source, that generates it, in space where the plants are situated.

2. The building-up of molecular formations containing the above elements.

3. Merging atoms and molecules into nanoparticles at cooling the gas mixture to normal temperature.

4. The movement of the nanoparticles formed in the gas medium.

5. The sedimentation of the nanoparticles on the plants.

6. The penetration of the nanoparticles inside the plant from its surface.

7. The movement of the nanoparticles inside the plant along its microchannels and through its pores, and through its cellular and intercellular spaces.

8. The decomposition of the nanoparticles inside the plant into the component molecules and atoms.
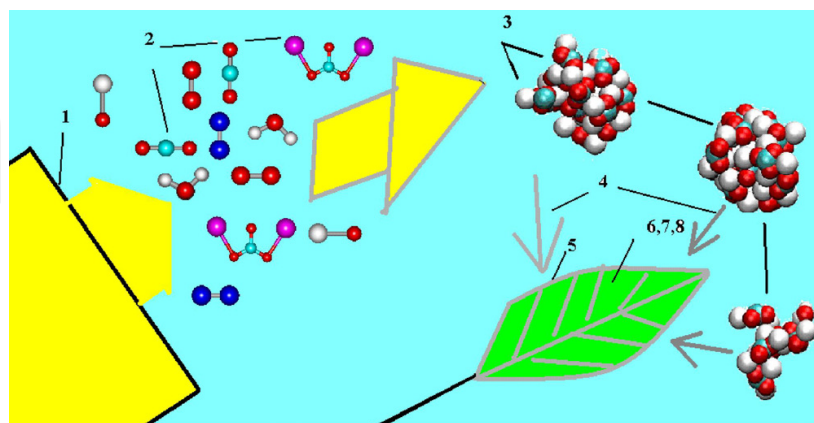
Figure 3. The main steps of the processes of the plant nutrition from the gas phase.

It should be noted that the tasks of modelling the processes of the plant nutrition from the gas phase are multilevel tasks, and each level requires special physical and mathematical approaches. Let us consider the methods for modelling the above successive processes. The calculation of the configuration of the molecular formations containing nitrogen, potassium and phosphorus (step 2) and the decomposition of the nanoparticles into component molecules and atoms inside the plant (step 8) require "ab initio" calculations. The simulation of the process of the molecule joining-up in nanoparticles at cooling the gas mixture to normal temperature (step 3) can be carried out with the help of the molecular dynamics methods. The calculation of the processes of the nanoparticle movement in the gas mixture, the sedimentation of the nanoparticles on the plant surface, the penetration of the nanoparticles inside the plant from its surface and the movement of the nanoparticles inside the plant along its microchannels, through its pores, cellular and intercellular spaces (steps 4–7) requires mesodynamics.

It is important that some of the processes could be considered within the framework of the continuum mechanics. They are the processes of the gas mixture movement over the space where the plants are (step 1) and steps 4 and 5 of the model under discussion as well. The theoretical base of multilevel simulation of the formation, movement, integration and disintegration of nanoparticles' systems in gas medium depending on the thermodynamic conditions of the medium are presented. The modelling is performed with the use of the methods of quantum mechanics, molecular dynamics and mesodynamics. As follows from the above-described process of application of nanoaerosols, nanoparticles are formed in a complex gas medium. Usually such problems are modeled by the molecular dynamics tools [6, 7]. However, their solution only within the framework of molecular dynamics requires much time and computational power. So, for example, due to a small mass of interacting atoms in order the integration scheme is stable the integration step should be taken of about 10^{-15} s, which leads to slow integration of the equations of molecular dynamics. Moreover, a collective behavior of atoms, molecules, and nanoparticles is observed at different

stages of application of nanoaerosols. This causes a multilevel character of the simulation problems to which there correspond different physical and mathematical approaches [8, 9]. The main problems of such simulation are:

- multilevel related problems;
- large number of variables;
- change of scales both in space and time;
- characteristic times of the processes at different levels differ by orders of magnitude;
- change of problem variables at different levels of simulation;
- coordination of the boundary conditions in transition from one level of simulation to another with change in the problem variables;
- stochastic behavior of nanosystems.

This leads to the necessity of using different mathematical approaches and models at different levels of formation and application of nanoaerosols. Calculation of the configuration of molecular formations that constitute nanoparticles requires "ab initio" calculations, i.e., quantum-mechanical methods of simulation [10]. These methods model nanoobjects most fully and accurately, with account for quantum effects. However, they require huge computational resources. At present the application of quantum-mechanical methods of calculation to nanosystems is limited by a number of atoms that enter the nanosystem not higher than 1000–2000 atoms. The process of aggregation of molecules to nanoparticles can be calculated by the methods of molecular dynamics [11–13]. These methods allow one to consider the systems that involve 10 and more millions of atoms but they do not take into account quantum phenomena.

Calculation of the motion processes of nanoparticles in a gas mixture and their aggregation is the problem of mesodynamics [14, 15]. A characteristic feature of mesodynamics is simultaneous use of the methods of molecular and classical dynamics. One should also mention that a number of processes, especially those occurring at the completing stages of nanoaerosol technologies, can be considered within the framework of continuum mechanics. Each method mentioned has its advantages and limitations. The use of one or another method of simulation or their combination as applied to specific problems of aerosol nanotechnology depends on the required accuracy of calculations. The main reasons and aims of transition from one method of simulation to another at different stages of nanoaerosol technologies are:

1. Decrease of the number of nanosystem variables due to transition from calculation of motion of separate atoms to the analysis of motion of nanoparticles or groups of them.
2. Decrease of the number of bonds between different elements of the nanosystem due to a decrease of the number of "nearest neighbors" occurring in the region of interaction of elementary cells of the nanosystem.
3. Increase of the computational size of the nanosystem due to enlargement of the elementary reference cell.
4. Broadening of the scale of nanosystem calculation in time due to an increase of the time step of integration of the nanosystem equations.

We consider the above-presented methods of simulation step by step and indicate the methods of the correlated application of them to different stages of the problems of aerosol nanotechnologies.

2.1. Quantum-chemical methods of simulation

Quantum-chemical methods of simulation use the quantum mechanics tools and are based on the solution of the Schrödinger equation [16]. In using this method one considers a full electronic and atomic structure of objects (atoms, molecules, ions), takes into account a detailed configuration of all electron clouds. In this case, complete information on the behavior of the considered system of N particles (nuclei of atoms and electrons) in the system of coordinates x_1, x_2, x_3 is determined by the wave function Ψ that depends on $3N$ coordinates of all particles of the atomic system, projections of their spines on the axis and time t

$$\Psi = \Psi \left(x_{11}, x_{21}, x_{31}, s_{x_{31}}, x_{12}, x_{22}, x_{32}, s_{x_{32}}; ...; x_{1N}, x_{2N}, x_{3N}, s_{x_{3N}}, t \right). \tag{1}$$

Variation of the wave function Ψ in space and time is determined by the Schrödinger wave equation

$$\mathbf{i}\, h \frac{\partial \Psi}{\partial t} = \widehat{\mathbf{H}} \Psi, \tag{2}$$

where h is the Planck constant; $\mathbf{i} = \sqrt{-1}$;

$$\widehat{\mathbf{H}} = \sum_{k=1}^{N} \left\{ -\frac{h^2}{2m_k} \nabla_k^2 + U_k \left(x_{1k}, x_{2k}, x_{3k}, s_{x_{3k}}, t \right) \right\} +$$

$$+ \sum_{k=1}^{N} \sum_{j \neq k=1}^{N} U_{kj} \left(x_{1k}, x_{2k}, x_{3k}, s_{x_{3k}} x_{1j}, x_{2j}, x_{3j}, s_{x_{3j}}, t \right) \tag{3}$$

where $\widehat{\mathbf{H}}$ is the Hamilton operator (an analogue of the classical Hamilton function) for the considered atomic system, $U_k \left(x_{1k}, x_{2k}, x_{3k}, s_{x_{3k}}, t \right)$ is the potential of the external field that acts on the kth particle, and $U_{kj} \left(x_{1k}, x_{2k}, x_{3k}, s_{x_{3k}} x_{1j}, x_{2j}, x_{3j}, s_{x_{3j}}, t \right)$ is the potential of interaction between the particles j and k.

Equation (3) holds when two conditions are met: elementary particles do not disappear and no new elementary particles appear in the evolution process of the nanosystem; the velocity of elementary particles is small compared with the velocity of light. For an aerosol nanosystem containing N^a atomic nuclei and N^el electrons the Hamilton operator (in the stationary case without account for spines of electrons) has the form

$$\widehat{\mathbf{H}} = -\widehat{\mathbf{K}}_{N^a} - \widehat{\mathbf{K}}_{N^{el}} + U_{N^a N^a} + U_{N^a N^{el}} + U_{N^{el} N^{el}}, \tag{4}$$

where

$$\widehat{\mathbf{K}}_{N^a} = -\frac{h^2}{2m_i} \sum_{i=1}^{N^a} \nabla_k^2 \tag{5}$$

is the operator of the kinetic energy of atomic nuclei,

$$\widehat{\mathbf{K}}_{N^{el}} = -\frac{h^2}{2m_{el}} \sum_{i=1}^{N^{el}} \nabla_k^2 \tag{6}$$

is the operator of the kinetic energy of electrons,

$$U_{N^a N^a} = e^2 \left(\sum_{l=1}^{N^a} \sum_{k=1, k \neq l}^{N^a} \frac{Z_k Z_l}{r_{kl}} \right) \tag{7}$$

is the potential energy of interaction of atomic nuclei,

$$U_{N^a N^{el}} = e^2 \left(\sum_{k=1}^{N^a} \sum_{i=1}^{N^{el}} \frac{Z_k}{r_{ik}} \right) \tag{8}$$

is the potential energy of interaction between the nuclei of atoms and electrons,

$$U_{N^{el} N^{el}} = e^2 \left(\sum_{i=1}^{N^{el}} \frac{1}{r_{ij}} \right) \tag{9}$$

is the potential energy of interaction of electrons; e is the electron charge, m_{el} is the electron mass, Z_k, Z_l is the number of protons in the atomic nucleus, r_{kl}, r_{ik}, r_{ij} are the distances between the atomic nuclei, between the nuclei of atoms and electrons, and between the electrons, respectively. With account for (5)–(9) the Hamilton operator (3) takes the form

$$\widehat{\mathbf{H}} = -\frac{h^2}{8\pi m_{el}} \sum_{i=1}^{N^{el}} \nabla_k^2 - \frac{h^2}{8\pi m_i} \sum_{i=1}^{N^a} \nabla_k^2 - e^2 \left(\sum_{k=1}^{N^a} \sum_{i=1}^{N^{el}} \frac{Z_k}{r_{ik}} - \sum_{i=1}^{N^{el}} \frac{1}{r_{ij}} - \sum_{l=1}^{N^a} \sum_{k=1, k \neq l}^{N^a} \frac{Z_k Z_l}{r_{kl}} \right). \tag{10}$$

In the general case, the Schrödinger equation does not have an analytical solution and is usually solved by numerical methods. Here, the main specific feature of the Schrödinger equation is that the function exists only for the entire system as a whole. An individual particle (atomic nucleus or electron) cannot be in the state which can be described by the wave function for a separate particle and the common wave function cannot be presented as a product of wave functions of separate particles. Therefore, direct solution of the Schrödinger equation requires huge computational capacities of computers. For the considered nanosystem consisting of atomic nuclei N^a and N^{el} electrons, the Schrödinger function should be determined in the configuration space $3N^a N^{el}$ dimensions. With a number of integration points over each dimension equal to 10^n, summation should be made by 10^f elements of the volume of the configuration space, where $f = 3nN^a N^{el}$. It is obvious that this is a very large number even for a small object. For example, for a nanoparticle containing 100 atoms and 100 electrons for 100 integration points over each coordinate the number of elements of the volume of the configuration space is 10^{60000}. At present the main efforts of researches are directed to the development of approximate calculation methods which will be considered during calculation of specific nanosystems.

2.2. Methods of molecular dynamics

Molecular dynamics, as applied to nanoaerosol technologies, can be successfully used for formation of the spatial structure and molecular atomic composition of nanoparticles which condense in gas mixture cooling. The molecular dynamics method was developed in the works by Hill, Dostovsky, Hughes, Ingold, Westheimer, Meyer, Alter, Older Vineyard, and other scientists in the period from 1946 to 1960 [17], and was intensely developed by the efforts of many scientists applied to different problems of simulating the processes in condensed, liquid, and gas media at the atomic level. This method is based on the concept of the Born-Oppenheimer force surface that is a multidimensional space describing the system energy as a function of the position of nuclei and atoms that form the system [17]. Thus, in the molecular dynamics method motion only of atomic nuclei of the nanosystem, but not the motion of electrons, is considered. The motion of atomic nuclei is determined by the Hamilton equations

$$\frac{d\bar{\mathbf{x}}_i}{dt} = \frac{\partial \mathbf{H}}{\partial \bar{\mathbf{p}}_i}, \tag{11}$$

$$\frac{d\bar{\mathbf{p}}_i}{dt} = -\frac{\partial \mathbf{H}}{\partial \bar{\mathbf{x}}_i}, \tag{12}$$

where

$$\mathbf{H} = \sum_{k=1}^{N} \left\{ \frac{p_k^2}{2m_k} + U_k\left(x_{1k}, x_{2k}, x_{3k}, t\right) \right\} +$$
$$+ \sum_{k=1}^{N} \sum_{j \neq k=1}^{N} U_{kj}\left(x_{1k}, x_{2k}, x_{3k}, x_{1j,2j}, x_{3j}, t\right) - \sum_{k=1}^{N} \alpha_k \bar{\mathbf{p}}_k \bar{\mathbf{x}}_k \tag{13}$$

is the Hamilton function, $\bar{\mathbf{x}}_i$ is the vector of the coordinates (x_{1i}, x_{2i}, x_{3i}), and $\bar{\mathbf{p}}_i$ is the vector of moment $\left(m_i \frac{dx_{1i}}{dt}, m_i \frac{dx_{2i}}{dt}, m_i \frac{dx_{3i}}{dt}\right)$.

Having substituted (13) into Eqs. (11) and (12), we obtain the equations of the motion of nanosystem atoms in the form of the Newton equations

$$m_i \frac{d\bar{\mathbf{V}}_i}{dt} = \sum_{j=1}^{N^a} \bar{\mathbf{F}}_{ij} + \bar{\mathbf{F}}_i^g\left(t\right) - \alpha_i m_i \bar{\mathbf{V}}_i, i = 1, 2, .., N^a, \frac{d\bar{\mathbf{x}}_i}{dt} = \bar{\mathbf{V}}_i, \tag{14}$$

where m_i is the mass of the ith atom, $\bar{\mathbf{F}}_{ij}$ are the forces of interatomic interaction, α_i is the coefficient of "friction" in the atomic system, $\bar{\mathbf{F}}_i^g\left(t\right)$ are the external forces, and t is the time.

As a rule, a random force $\bar{\mathbf{F}}_i^g\left(t\right)$ that affects the ith atom and is specified by the Gauss distribution. The Gauss distribution is the δ-correlated in time Gaussian random process with the following properties:

a mean value of the random force is 0

$$\left\langle \bar{\mathbf{F}}_i^g\left(t\right) \right\rangle = 0; \tag{15}$$

$\bar{\mathbf{F}}_i^g(t)$ does not correlate with the velocity $\frac{d\bar{\mathbf{x}}_i}{dt}$ of the atom under consideration, thus

$$\left\langle \bar{\mathbf{F}}_i^g(t) \frac{d\bar{\mathbf{x}}_i}{dt} \right\rangle = 0; \tag{16}$$

$$\left\langle \bar{\mathbf{F}}_i^g(t) \bar{\mathbf{F}}_i^g(0) \right\rangle = 2k_B T_0 \alpha_i m_i \delta(t), \tag{17}$$

where k_B is the Boltzmann constant, $\delta(t)$ is the Dirac delta function, and T_0 is the temperature. Thus, the interaction of the atomic molecular system with the external medium (the heat reservoir), which consists of the following two parts: the systematic friction force

$$\sum_{j=1}^{N^a} \bar{\mathbf{F}}_i^f(t) = -\alpha_i m_i \bar{\mathbf{V}}_i, \tag{18}$$

and the random force $\bar{\mathbf{F}}_i^g(t)$ (noise) is described. In this case, the equations of motion are called the Langevin equations and the molecular dynamics method of calculation by these equations is given the name of the Langevin dynamics method.

Nanoparticles start formation from the gas medium that at the initial instant consists of the atoms of different materials and molecules. In cooling, due to condensation the gas medium is supplemented with time by nanoparticles. This process occurs in a macro-volume including a large number of atoms and molecules. Simulation of such system by the methods of molecular dynamics is impossible due a large number of variables, therefore simulation occurs in a calculated cell occupying nano- or microvolume with the specific boundary conditions of the Born-Karman surface of the cell [7, 17]. In this case, the molecular dynamics tools allow obtaining of not only general characteristics of the system, but also make it possible to follow the trajectories of each atom and nanoparticle. The essence of these boundary conditions is explained in Figure 4. The space modeled is divided to 27 equal cells. The central cell is the calculated cell, other cells are the "images" of it. In this case, simulation is made in the central cell only. All other cells-images contain the same set of atoms, molecules and nanoparticles as the calculated cell has. The total number of the images of the calculated cell is 26. The molecular dynamics equations (14) are written only in the calculated cell. The trajectories of motion of atoms, molecules, and nanoparticles in the images of the calculated cell are specified by absolutely similar trajectories of their motion in the calculated cell according to Eqs. (14).

When any atom, molecule, or nanoparticle from the inner space crosses any boundary, a similar atom, molecule, or nanoparticle with the same properties and velocity appears in the calculated cell from the opposite boundary. When an atom, molecule, or nanoparticle approaches the inner boundary of the cell the atoms, molecules, and nanoparticles of the images begin to affect them. Thus, the entire calculated space is presented in the form of the set of equal calculated volumes and motion of microobjects and occurrence of any processes in them are taken to be identical and the effect of the calculated cell edges is eliminated. Thanks to the hypothesis on the periodicity of the modeled region, the periodic boundary conditions allow a decrease of the calculated volume and, thus, a considerable decrease of the computation expenses in simulation. We consider a mathematical formulation of the Born-Karman periodic boundary conditions. A set of images of the ith atom with the
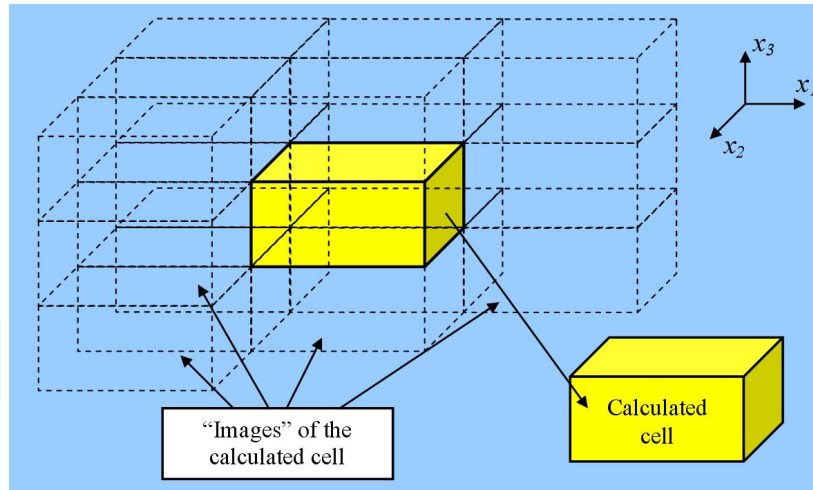
Figure 4. Periodic boundary conditions.

coordinate $\bar{\mathbf{r}}_i$ is specified as follows:

$$\bar{\mathbf{r}}_{i,image(k_1,k_2,k_3)} = \bar{\mathbf{r}}_i + L_j \cdot \bar{\mathbf{i}}_j, \ k_1, k_2, k_3 = 1, 2, 3, \tag{19}$$

where L_j is the length of the calculated cell along the corresponding coordinate, k_1, k_2, k_3 are the numbers of cells-images in all directions, $\bar{\mathbf{r}}_{i,image(k_1,k_2,k_3)}$ is the radius-vector of the image of ith atom, and $\bar{\mathbf{i}}_j$ is the transfer vector;

$$\bar{\mathbf{i}}_j = \begin{pmatrix} i_1 \\ i_2 \\ i_3 \end{pmatrix}, \ i_1, i_2, i_3 = \text{-} 1, 0, 1, \ i_1 \neq i_2 \neq i_3 = 0, \tag{20}$$

In such a manner we create all 26 images of the ith atom. As the atom reaches the boundary of the calculated cell it enters the cell from the opposite side with the coordinates $\bar{\mathbf{r}}_i = \bar{\mathbf{r}}_i^* + L_j \cdot \bar{\mathbf{l}}_j$, where

$$\bar{\mathbf{l}}_j = \begin{pmatrix} l_1 \\ l_2 \\ l_3 \end{pmatrix}, \ l_1, l_2, l_3 = \text{-} 1, 0, 1, \ l_1 \neq l_2 = \pm 1, \ l_2 \neq l_3 = \pm 1, \ l_1 \neq l_3 = \pm 1, \tag{21}$$

$\bar{\mathbf{r}}_i^*$ is the radius-vector of the ith atom at the boundary of the calculated cell and $\bar{\mathbf{l}}_j$ is the transfer vector. The atom preserves the motion parameters:

$$\bar{\mathbf{V}}(\bar{\mathbf{r}}_i) = \bar{\mathbf{V}}(\bar{\mathbf{r}}_i^* + L_j \cdot \bar{\mathbf{l}}_j). \tag{22}$$

The presented mathematical formulation of the periodic boundary conditions eliminates the effect of edges and allows one to accurately describe interactions occurring in the calculated region. To calculate the problem of nanoparticles formation in the calculated cell by the molecular dynamics method we use the structure of molecules constituting the gas mixture, which is obtained at the first stage of simulation, and specify the coordinates and velocities of atoms of all molecules at the time instant $t = 0$

$$\bar{\mathbf{x}}_i = \bar{\mathbf{x}}_{i0}, \frac{d\bar{\mathbf{x}}_i}{dt} = \bar{\mathbf{V}}_i = \bar{\mathbf{V}}_{i0}, \ t = 0, \bar{\mathbf{x}}_i \subset \Omega, \tag{23}$$

where Ω is the volume of the calculated cell. The initial coordinates of atoms and molecules $\bar{\mathbf{x}}_{i0}$ are specified proceeding from the uniform distribution of them in the gas mixture and random mixing within the calculated cell. Modules of the initial velocities of atoms and molecules are calculated according to the Maxwell distribution [17] proceeding from the initial temperature of the gas mixture T_0. The relation between the initial temperature T_0 and initial velocities $\bar{\mathbf{V}}_{i0}$ is determined by the expression

$$T_0 = \frac{1}{3Nk_B} \sum_{i=1}^{N_a} m_i \left(\bar{\mathbf{V}}_{i0}\right)^2,$$

(24)

where N is the total number of the degrees of freedom of the atoms in the gas mixture and N_a is the number of atoms in the gas mixture. The Maxwell distribution for the velocity vector $\bar{\mathbf{V}}_0 = \left(\bar{\mathbf{V}}_{x0}, \bar{\mathbf{V}}_{y0}, \bar{\mathbf{V}}_{z0}\right)$ is the product of the distributions for each of three directions:

$$f_V \left(\bar{\mathbf{V}}_{x0}, \bar{\mathbf{V}}_{y0}, \bar{\mathbf{V}}_{z0}\right) = f_V \left(\bar{\mathbf{V}}_{x0}\right) f_V \left(\bar{\mathbf{V}}_{y0}\right) f_V \left(\bar{\mathbf{V}}_{z0}\right),$$

(25)

where the distribution along one direction is determined by the normal distribution:

$$f_V \left(\bar{\mathbf{V}}_{x0}\right) = \sqrt{\frac{m}{2\pi k_b T_0}} \exp\left(-\frac{m(\bar{\mathbf{V}}_{x0})^2}{2k_b T_0}\right).$$

(26)

Integrating the system of equations (14) with respect for time using the presented initial conditions, at the time instant t we obtain the main parameters of nanoaerosol:

a mean kinetic energy of the system

$$E(t) = \frac{\sum\limits_{i=1}^{N} m_i \left(\bar{\mathbf{V}}_i(t)\right)^2}{2},$$

(27)

an instantaneous value of temperature

$$T(t) = \frac{1}{3Nk_B} \sum_{i=1}^{N} m_i \left(\bar{\mathbf{V}}_i(t)\right)^2.$$

(28)

The temperature is obtained by averaging of the instantaneous values $T(t)$ over some time range

$$T(t) = \frac{1}{3Nk_B\tau} \int_{t_0}^{t_0+\tau} \sum_{i=1}^{n} m_i \left(\bar{\mathbf{V}}_i(t)\right)^2 dt.$$

(29)

Under real conditions the molecular system usually exchanges energy with the surrounding. Special algorithms - thermostats - are used to take into account such energy interactions. The use of the thermostat allows one to calculate molecular dynamics at a constant temperature of the medium or, on the contrary, to change the medium temperature according to a certain law.

In the general case, the thermostat temperature does not coincide with the temperature of the molecular system. At a fixed temperature of the thermostat the molecular system temperature

can change due to different reasons. In the case of the established equilibrium, the thermostat temperature and the mean temperature of the molecular system should coincide. The simplest way to maintain a constant temperature of the thermostat is scaling of velocities. Scaling is done using the expression

$$\bar{\mathbf{V}}_j^{new}(t) = \bar{\mathbf{V}}_j^{old}(t) \cdot \sqrt{3Nk_BT_t \Big/ \left\langle \sum_{i=1}^{N} m_i \left(\bar{\mathbf{V}}_i^{old}(t)\right)^2 \right\rangle}, \tag{30}$$

where T_t is the thermostat temperature. Averaging of a value of the total moment within the time interval between scaling of velocities is denoted in angular brackets. Another important factor is the effect of the initial temperature on the distribution of molecule velocities. As is shown above, in the molecular dynamics problem the velocity field at the initial instant of time is usually selected according to the Maxwell distribution. This distribution has a form of normal distribution. As should be expected, for gas at rest a mean velocity in any direction is zero. It is of interest to know the distribution of the velocities of molecules or atoms not over the projections but over the absolute value of velocities. The velocity modulus V is determined as

$$V = \sqrt{V_{x_1}^2 + V_{x_2}^2 + V_{x_3}^2}. \tag{31}$$

Therefore, the velocity modulus will always be larger than or equal to zero. Since all V_j are distributed normally, V^2 will have the $f(V)$ distribution with three degrees of freedom. If $f(V)$ is the probability density function for the velocity modulus, then it has the form:

$$f(V)\, dV = 4\pi V^2 \left(\frac{m_i}{2\pi k_B T}\right)^{3/2} \exp\left(\frac{-m_i V^2}{2k_B T}\right) dV. \tag{32}$$

The following expression is used for calculation of the nanosystem pressure:

$$P(t) = \frac{1}{3W} \left[\sum_{i=1}^{N} m_i \left(\bar{\mathbf{V}}_i(t)\right)^2 - \sum_{i,j;i<i} \left(\bar{\mathbf{r}}_{\tilde{j}}(t) - \bar{\mathbf{r}}_i(t)\right) \bar{\mathbf{F}}_{i\tilde{j}}(t) \right], \tag{33}$$

where W is the volume occupied by the nanosystem. The first term in (33) depends on the energy of motion of atoms or molecules and the second term is determined by pairwise interaction of atoms. Along with the pair of ith and jth atoms, all images of the jth atom are considered and interaction between the closest image $\tilde{j}$ and the ith atom is calculated. The function $\bar{\mathbf{F}}_{i\tilde{j}}(t)$ characterizes a value of interaction between the atoms. The use of the barostat algorithms allows simulation of the behavior of the system at constant pressure. The simplest of them is the Berendsen barostat where a value of pressure is maintained constant by scaling the calculated cell. The position of the particles in the system at each time step is modified according to the scaling coefficient of the Berendsen barostat μ:

$$\bar{\mathbf{r}}_i(t) \rightarrow \mu\bar{\mathbf{r}}_i(t),\ i = 1, 2, ..., N. \tag{34}$$

The scaling coefficient is determined by the expression

$$\mu = \sqrt[3]{1 - \frac{\Delta t}{\tau_P} (P - P_b)},$$ (35)

where Δt is the integration step, τ_P is the time of barostat implementation, P is the current pressure, and P_b is the barostat pressure. Transformation of the position of particles by formula (34) leads to the change of the calculated cell size and volume and thus to the change of pressure. The primary problem of the molecular dynamics method is calculation of the forces of interaction between atoms (molecules). Forces of this interaction are potential and are determined from the expression

$$\bar{\mathbf{F}}_{ij} = - \sum_{i=1}^{N} \frac{\partial U(\bar{\mathbf{r}})}{\partial \bar{\mathbf{r}}_i} ,$$ (36)

where $\bar{\mathbf{r}} = \{\bar{\mathbf{r}}_1, \bar{\mathbf{r}}_2, ..., \bar{\mathbf{r}}_N\}$; $\bar{\mathbf{r}}_i$ is the radius vector of the ith atom, is the potential of intramolecular interaction that depends on the mutual position of all atoms. This method is based on the concept the Born-Oppenheimer force surface that is the multidimensional space describing the system energy as a function of the position of the nuclei of atoms that form it [17]. The potential $U(\bar{\mathbf{r}})$, in the general case, is specified in the sum of several components that correspond to different types of interaction:

$$U(\bar{\mathbf{r}}) = U_b + U_\theta + U_\varphi + U_{ej} + U_{LJ} + U_{es} + U_{hb},$$ (37)

where the terms correspond to the following types of interactions: the change of the bond length U_b, the change of bond angle U_θ, the torsion angles U_φ, the plane groups U_{ej}, the van-der-waals interactions U_{LJ}, the electrostatic interactions U_{es}, and the hydrogen bonds U_{hb}. The indicated terms have different functional forms [11].

2.3. Simulation of nanosystems by mesodynamics methods

Calculations of controlled gas media by the molecular dynamics method are effective at the initial stage of formation of nanoparticles. However, simulation of processes that occur in the gas medium by molecular dynamics at the atomic level requires huge computer resources and time. This stipulates the topicality of the development of economic methods of calculation. In this section, we suggest a technique that is based on the mesodynamics methods [18]. We note that mesodynamics is the development of method of particles. The essence of the method is as follows. As atoms and molecules merge to nanoparticles, the larger number them manifest a collective behavior. Atoms and molecules making the nanoparticle move together with small oscillation near the equilibrium position within the nanoparticle structure. This allows one to decrease a number of simulated objects and to use another simulation method – mesodynamics. Mesodynamics is based on a collective behavior of atoms and uses force parameters that are calculated by the molecular dynamics methods. In this case, motion of nanoparticles is studied by the methods of classical mechanics. We consider main stages of application of mesodynamics.

The first stage is the calculation of interaction of the pair of nanoparticles. We give the problem formulation for symmetric nanoparticles and then for nanoparticles of an arbitrary shape. With this in mind, we consider a nanoparticle that consists of N^a atoms occupying the region Ω at the time instant $t = 0$ (Figure 5). The position of each ith atom of the nanoelement is specified by the coordinates x_{i1}, x_{i2}, x_{i3}. Atoms interact with each other. Figure 6 shows the interaction forces $\bar{\mathbf{F}}_{ik}$ (the force of interaction between atoms i and k) and $\bar{\mathbf{F}}_{ij}$ (the force of interaction between atoms i and j). The force of interaction between two atoms is directed along the line that connects their centers. Moreover, each ith atom of the nanoelement is affected by the external force $\bar{\mathbf{F}}_i^b$. The direction and value of this force is determined by the type of interaction between the nanoelement and the surrounding medium. Atoms of a nanoparticle move under the action of the system of these forces.
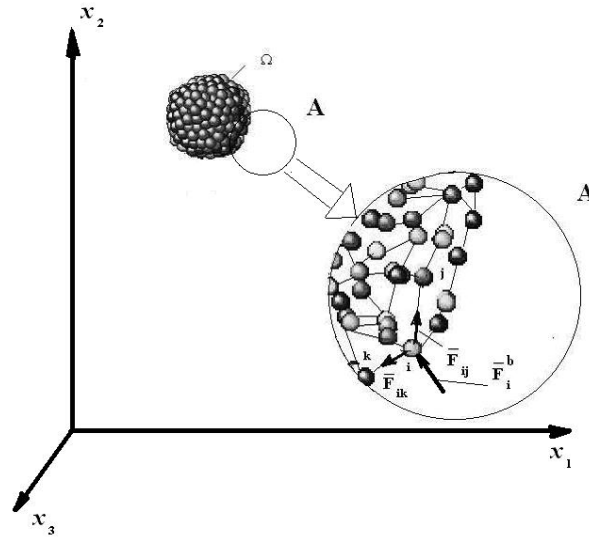
Figure 5. Nanoparticle: A) Magnified image of the part of a nanoparticle.

The motion of atoms that form a nanoparticle is determined, according to the molecular dynamics method, by the system of differential equations (14) which is supplemented with forces caused by interactions of atoms with the surrounding medium

$$\bar{\mathbf{F}}_{bi} = -\sum_1^N \frac{\partial U_b(\rho_{bi})}{\partial \rho_{bi}} \, \bar{\mathbf{e}}_{ib}, \tag{38}$$

where ρ_{bi} is the distance between atom i and atom b from the surrounding medium, $\bar{\mathbf{e}}_{ib}$ is the unit vector directed from atom i to atom b, and $U_b(\rho_{bi})$ is the potential of interaction between nanoparticle atoms and atoms from the surrounding medium. We consider two symmetric nanoparticles lying at a distance S from each other (Fig. 4). In this case, Eq. (14) takes the form

$$m_i \frac{d^2 \bar{\mathbf{x}}_i}{dt^2} = \sum_{j=1}^{N_1+N_2} \bar{\mathbf{F}}_{ij} + \bar{\mathbf{F}}_i(t) - \alpha_i m_i \frac{d\bar{\mathbf{x}}_i}{dt}, \ i = 1, 2, ..., (N_1 + N_2), \tag{39}$$

at the boundary conditions

$$\bar{\mathbf{x}}_i = \bar{\mathbf{x}}_{i0}, \bar{\mathbf{V}}_i = \bar{\mathbf{V}}_{i0}, \ t = 0, \ \bar{\mathbf{x}}_i \subset \Omega_1 \bigcup \Omega_2, \tag{40}$$

where N_1 and N_2 is the number of atoms in the first and second nanoparticles, respectively, Ω_1 and Ω_2 are the regions occupied by the first and second nanoparticles, respectively. Solution of (39) at the boundary conditions (40) allows calculation of the trajectories of motion of atoms of each nanoparticle and, consequently, of nanoparticles as a whole. In this case, the total forces of interaction between the particles will be determined by the relation

$$\bar{\mathbf{F}}_{b1} = -\bar{\mathbf{F}}_{b2} = \sum_{i=1}^{N_1} \sum_{j=1}^{N_2} \bar{\mathbf{F}}_{ij}, \tag{41}$$

where i and j are the atoms of the first and second nanoparticles, respectively.
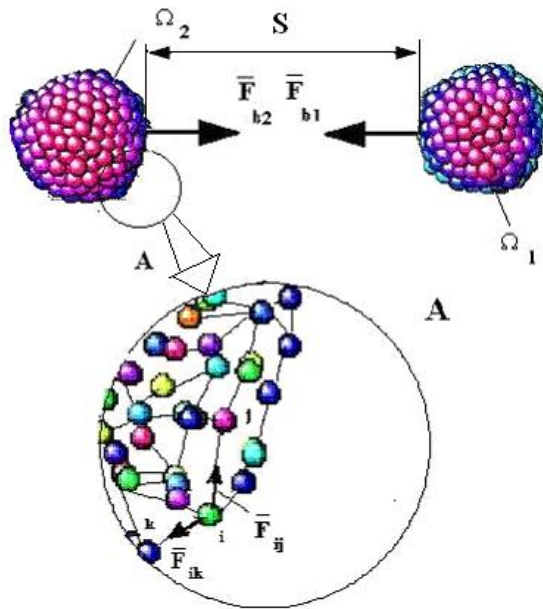
Figure 6. Schematic of interaction of nanoparticles: A) Magnified image of the part of a nanoparticle.

In the general case, the force of interaction of nanoparticles $\bar{\mathbf{F}}_{bi}$ can be written as the product of functions dependent on the size of nanoparticles and the distance between them:

$$|\bar{\mathbf{F}}_{bi}| = \Phi_{11}(S_c) \cdot \Phi_{12}(D). \tag{42}$$

The direction of the vector $\bar{\mathbf{F}}_{bi}$ is determined by the director cones of the vector that connects the centers of masses of nanoparticles. Of course, the forces of interaction between the particles change in time with small oscillations about a mean value. Therefore, Eq. (42) determines a mean value of the interaction force of nanoparticles. We consider two interacting nonsymmetric nanoparticles lying from one another at a distance S_c between their centers of masses and oriented at certain specified angles relative to one another (Figure 7). In contrast to the previous problem interaction of atoms entering into nanoparticles leads not only to relative displacement, but to rotation of the latter. Thus, in the general case, the sum of all forces of interaction of atoms of the nanoelements is reduced to the resultant vector of forces

$\overline{\mathbf{F}}$ and the principal moment $\overline{\mathbf{M}}$

$$\overline{\mathbf{F}} = \overline{\mathbf{F}}_{b1} = -\overline{\mathbf{F}}_{b2} = \sum_{i=1}^{N_1} \sum_{j=1}^{N_2} \overline{\mathbf{F}}_{ij}, \tag{43}$$

$$\overline{\mathbf{M}} = \overline{\mathbf{M}}_{b1} = -\overline{\mathbf{M}}_{b2}, \tag{44}$$

where i and j are the atoms of the first and second nanoparticles, respectively.
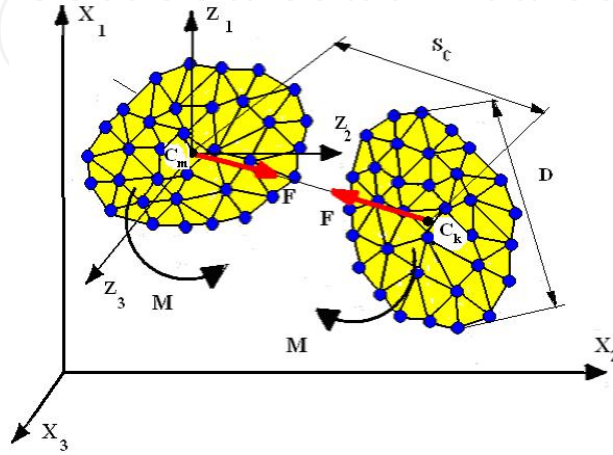
Figure 7. Interacting nanoparticles: $\overline{\mathbf{M}}, \overline{\mathbf{F}}$ are the principal moment and resultant vector of forces.

The main aim of this stage of calculation is the construction of the dependences of forces and momenta of interaction of nanoparticles on the distance between their centers of masses S_c, angles of mutual orientation of nanoparticles $\Theta_1, \Theta_2, \Theta_3$ (shape of a nanoelement), and their characteristic dimension D. In the general case, these dependences can be presented in the form

$$\bar{\mathbf{F}}_{bi} = \bar{\Phi}_1(S_c, \Theta_1, \Theta_2, \Theta_3, D), \tag{45}$$

$$\bar{\mathbf{M}}_{bi} = \bar{\Phi}_2(S_c, \Theta_1, \Theta_2, \Theta_3, D). \tag{46}$$

For spherical nanoparticles the angles of mutual orientation do not influence the force of their interaction, therefore the moment in Eq. (39) is identically equal to zero. In the general case, functions (45) and (46) can be approximated, by analogy with (42), as a product of the functions of $S_c, \Theta_1, \Theta_2, \Theta_3, D$, respectively. In the study of the evolution of the system of interacting nanoparticles we consider motion of each nanoparticle as a comprehensive whole. In this case the translatory motion of the center of masses of each nanoparticle is specified in the system of X_1, X_2, X_3, and rotation of a nanoparticle is described in the system of coordinates Z_1, Z_2, Z_3 related to its center of masses (Figure 8).

This transition allows one to pass to other variables (from the coordinates and velocities of atoms to the coordinates and velocities of the center of masses of nanoparticles) and to decrease the number of them. For a nanosystem consisting of N^{np} nanoparticles each of which contains N^a atoms the number of mesodynamics variables, compared to the molecular dynamics method, decrease k_x times, which is calculated by the formula [15]

$$k_x = \xi_x \frac{N^a N^{np}}{N^{np}} = \xi_x N^a, \tag{47}$$
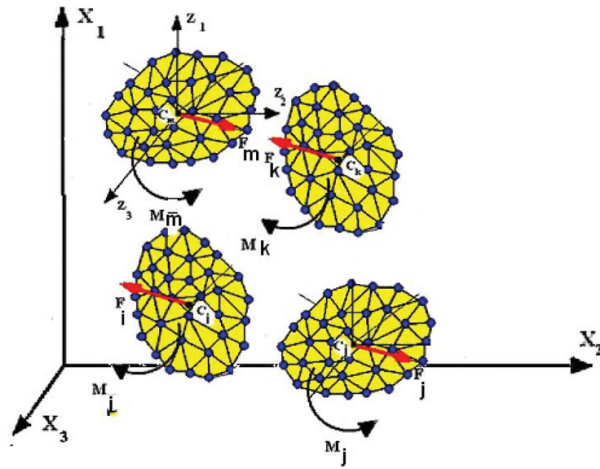
Figure 8. System of interacting particles.

where $\xi_x = 1$ for force interaction of nanoparticles, $\xi_x = 0.5$ when both forces and momenta of interaction of nanoparticles are taken into account. The system of equations that describes motion of interacting nanoparticles has the form

$$
\begin{cases}
M_k \frac{d^2 X_1^k}{d t^2} = \sum\limits_{j=1}^{N_e} F_{X_1}^{kj} + F_{X_1}^{ke}, \\[2mm]
M_k \frac{d^2 X_2^k}{d t^2} = \sum\limits_{j=1}^{N_e} F_{X_2}^{kj} + F_{X_2}^{ke}, \\[2mm]
M_k \frac{d^2 X_3^k}{d t^2} = \sum\limits_{j=1}^{N_e} F_{X_3}^{kj} + F_{X_3}^{ke}, \\[2mm]
J_{Z_1}^k \frac{d^2 \Theta_1^k}{dt^2} + \frac{d\Theta_2^k}{dt} \cdot \frac{d\Theta_3^k}{dt} (J_{Z_3}^k - J_{Z_2}^k) = \sum\limits_{j=1}^{N_e} M_{Z_1}^{kj} + M_{Z_1}^{ke}, \\[2mm]
J_{Z_2}^k \frac{d^2 \Theta_2^k}{dt^2} + \frac{d\Theta_1^k}{dt} \cdot \frac{d\Theta_3^k}{dt} (J_{Z_1}^k - J_{Z_3}^k) = \sum\limits_{j=1}^{N_e} M_{Z_2}^{kj} + M_{Z_2}^{ke}, \\[2mm]
J_{Z_3}^k \frac{d^2 \Theta_3^k}{dt^2} + \frac{d\Theta_2^k}{dt} \cdot \frac{d\Theta_1^k}{dt} (J_{Z_2}^k - J_{Z_1}^k) = \sum\limits_{j=1}^{N_e} M_{Z_3}^{kj} + M_{Z_3}^{ke},
\end{cases}
\tag{48}
$$

where X_i^k, Θ_i are the coordinates of the centers of masses and the orientation angles of the principle axes Z_1, Z_2, Z_3 of nanoaoparticles; $F_{X_1}^{kj}, F_{X_2}^{kj}, F_{X_3}^{kj}$ are the interaction forces of nanoparticles calculated by formulas (42) or (43); $F_{X_1}^{ke}, F_{X_2}^{ke}, F_{X_3}^{ke}$ are the external forces acting on nanoparticles; N_k is the number of nanoparticles; M_k is the nanoparticle; $M_{Z_1}^{kj}, M_{Z_2}^{kj}, M_{Z_3}^{kj}$ are the momenta of interaction forces of nanoparticles calculated by formulas (46); $M_{Z_1}^{ke}, M_{Z_2}^{ke}, M_{Z_3}^{ke}$ are external momenta acting on nanoparticles; $J_{Z_1}, J_{Z_2}, J_{Z_3}$ are inertia momenta of nanoparticles. The initial conditions for the system of equations (48) have the form

$$
\bar{X}^k = \bar{X}_0^k, \; \Theta^k = \Theta_0^k, \; \bar{V}^k = \bar{V}_0^k, \; \frac{d\Theta^k}{dt} = \frac{d\Theta_0^k}{dt}.
\tag{49}
$$

During the motion of nanoparticles a pair of nanoparticles can merge. In this case, a number of nanoparticles in the system decreases by unity and, correspondingly, the number of equations in the system (48) decreases by six. Thus, the parameters of a new, merged, nanoparticle is calculated and a new reduced system of equations is integrated. It should be noted that if the momenta of interaction of nanoparticles with each other and with the surrounding medium are zero, only the first three equations remain in the system of equations (48). Equations of the motion of nanoparticles (48) allow for all interactions between nanoparticles and their interactions with the surrounding medium. However, in the gas medium where nanoparticles are formed the distance between nanoparticles is large and interaction between nanoparticles is short-range. For this case, the system of equations (48) can be written as

$$\begin{cases} M_k \frac{d^2 X_1^k}{d\,t^2} = F_{X_1}^{ke}, \\ M_k \frac{d^2 X_2^k}{d\,t^2} = F_{X_2}^{ke}, \\ M_k \frac{d^2 X_3^k}{d\,t^2} = F_{X_3}^{ke}, \\ J_{Z_1}^k \frac{d^2 \Theta_1^k}{dt^2} + \frac{d\Theta_2^k}{dt} \cdot \frac{d\Theta_3^k}{dt}(J_{Z_3}^k - J_{Z_2}^k) = M_{Z_1}^{ke}, \\ J_{Z_2}^k \frac{d^2 \Theta_2^k}{dt^2} + \frac{d\Theta_1^k}{dt} \cdot \frac{d\Theta_3^k}{dt}(J_{Z_1}^k - J_{Z_3}^k) = M_{Z_2}^{ke}, \\ J_{Z_3}^k \frac{d^2 \Theta_3^k}{dt^2} + \frac{d\Theta_2^k}{dt} \cdot \frac{d\Theta_1^k}{dt}(J_{Z_2}^k - J_{Z_1}^k) = M_{Z_3}^{ke}. \end{cases} \tag{50}$$

If the moment and rotation of nanoparticles is disregarded, the system of equations (50) takes the form

$$\begin{cases} M_k \frac{d^2 X_1^k}{dt^2} = F_{X_1}^{ke}, \\ M_k \frac{d^2 X_2^k}{dt^2} = F_{X_2}^{ke}, \\ M_k \frac{d^2 X_3^k}{dt^2} = F_{X_3}^{ke}. \end{cases} \tag{51}$$

The forces of interaction of nanoparticles with the gas medium can be presented as

$$\bar{\mathbf{F}}_{X_i}^{ke}(t, \bar{\mathbf{r}}(t)) = -M_i g + \bar{\mathbf{f}}_i(t) - m_i b_i \frac{d\bar{\mathbf{X}}_i(t)}{dt}, \; i = 1,2,...,n, \tag{52}$$

where $\bar{\mathbf{f}}_i(t)$ is the random force acting on the ith nanoparticle from the side of the gas medium, b_i is the coefficient of "friction" in the nanoparticles-gas medium system. The random force $\bar{\mathbf{f}}_i(t)$ is similar to the random force in the Langevin dynamics. We note that the random force $\bar{\mathbf{f}}_i(t)$ reflects the effect of the gas phase molecules on nanoparticles moving in it. It is determined from the Gauss distribution with the following properties: a mean value of the random force $\bar{\mathbf{f}}_i(t)$ is zero and it correlates with the velocity $\bar{\mathbf{V}}_i(t)$ of the considered nanoparticle such that

$$\left\langle \overline{\mathbf{f}_i}(t)\bar{\mathbf{V}}_i(t) \right\rangle = 0, \; \left\langle \overline{\mathbf{f}_i}(t)\overline{\mathbf{f}_i}(0) \right\rangle = 2k_B T_0 b_i m_i \delta(t). \tag{53}$$

In order to model the random force fthe Box-Müller transformation is used in Eq. (52). Let x and y be independent random quantities uniformly distributed on the section $[-1, 1]$. We determine $R = x^2 + y^2$. In the case when $R > 1$ or $R = 0$, the values of x and y should be

generated anew. As soon as the condition $0 < R \leqslant 1$ is met, z_0 and z_1 are calculated. z_0 and z_1 are independent random quantities satisfying the standard normal distribution

$$z_0 = x\sqrt{\frac{-2\ln R}{R}}, \; z_1 = y\sqrt{\frac{-2\ln R}{R}}. \tag{54}$$
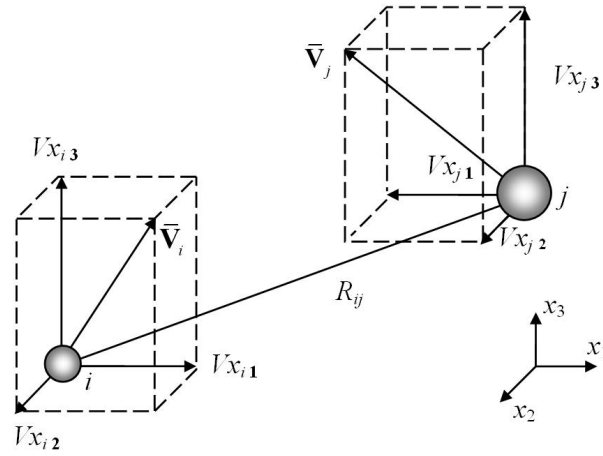
Figure 9. Mutual position of the ith and jth particles.

On obtaining the standard normal random quantity z, we can easily pass to the quantity $\xi\left(\mu, \sigma^2\right)$ distributed normally with the mathematic expectation μ and the standard deviation σ by the formula $\xi = \mu + \sigma z$. According to the data on the random force $\bar{\mathbf{f}}_i(t)$ in Eq. (52), it has the mathematical expectation $\mu = 0$ and standard deviation

$$\sigma = \sqrt{2k_B T_0 b_i m_i \delta\left(t\right)}. \tag{55}$$

The processes of condensation of nanoparticles in the gas medium are stipulated by the presence of potentials of interaction between the atoms. In the gas medium with nanoparticles two main factors affect the processes of their merging: the distance between the interacting particles and the direction and value of velocities. We consider two nanoparticles that are at a distance R_{ij} from each other at an arbitrary instant of time (Figure 9). When R_{ij} is small, the condition of "sticking" of nanoparticles is met. The second factor that affects condensation of nanoparticles is determined by the value and direction of velocities. It is obvious that very "fast" particles can overshoot one another even in contact. The angle α between the velocity vectors (Figure 10) that determines the direction of the motion of particles also substantially affects merging of particles.

The choice of an adequate condition of sticking of nanoparticles determines the processes of formation of new nanoparticles and the dynamics of their motion. The sticking criterion of nanoparticles can be presented in the form

$$\Phi(|R| - R_{ij}; \bar{\mathbf{V}}_i - \bar{\mathbf{V}}_j) = 0. \tag{56}$$

In the problem of merging of non-interacting nanoparticles of great importance is the choice of the correct time step of integration of Eqs. (51) in both analytical and numerical solution of them. The choice of a small time step increases the time of problem calculation. A very
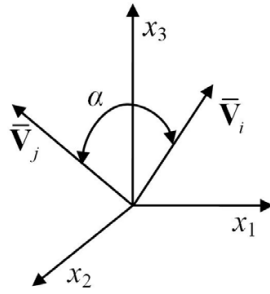
Figure 10. Velocity vectors of the ith and jth particles.

large integration step can lead to "overshoot" of nanoparticles despite condition (54). Thus, the problem of selecting an optimum time step arises. Solution of this problem in the present paper is based on the position of nanoparticles and values of their velocities. Figure 11 shows a pair of nanoparticles at some instant of time. Nanoparticles have the velocities $\bar{\mathbf{V}}_i$ and $\bar{\mathbf{V}}_j$ and their position is determined by the current radius vectors $\bar{\mathbf{r}}_i$ and $\bar{\mathbf{r}}_j$ respectively. The projections of the velocities of the ith and jth particles are determined according to the formulas

$$pr_{R_{ij}}\bar{\mathbf{V}}_i = \bar{\mathbf{V}}_i \cdot \bar{\mathbf{R}}_{ij}/R_{ij}, \ \ pr_{R_{ij}}\bar{\mathbf{V}}_j = \bar{\mathbf{V}}_j \cdot \bar{\mathbf{R}}_{ji}/R_{ij}. \tag{57}$$
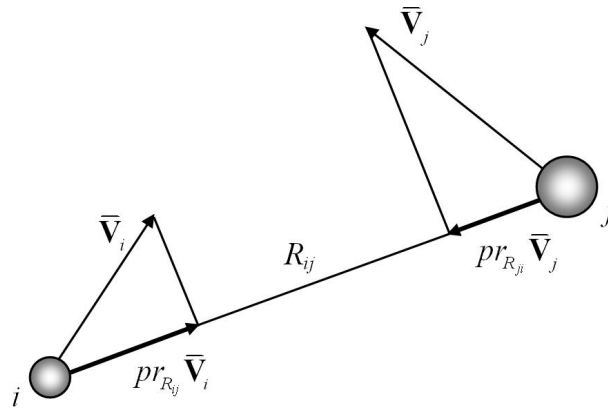
Figure 11. Two nanoparticles moving at the velocities $\bar{\mathbf{V}}_i$ and $\bar{\mathbf{V}}_j$.

The vectors $\bar{\mathbf{R}}_{ij}$, $\bar{\mathbf{R}}_{ji}$ and the distance between the particles R_{ij} are calculated from the relations

$$\bar{\mathbf{R}}_{ij} = \bar{\mathbf{r}}_j - \bar{\mathbf{r}}_i, \ \bar{\mathbf{R}}_{ji} = \bar{\mathbf{r}}_i - \bar{\mathbf{r}}_j, \ R_{ij} = \left|\bar{\mathbf{R}}_{ij}\right| = \left|\bar{\mathbf{R}}_{ji}\right| = \left|\bar{\mathbf{r}}_j - \bar{\mathbf{r}}_i\right|. \tag{58}$$

The time interval in which collision of the ith and jth particles becomes possible is directly proportional to the distance between the particles and inversely proportional to the velocity projections:

$$\Delta t_{ij} = \frac{R_{ij}}{pr_{R_{ij}}\bar{\mathbf{V}}_i + pr_{R_{ij}}\bar{\mathbf{V}}_j}. \tag{59}$$

Using formula (59), by selection of all possible pairs of particles, one finds the smallest positive value Δt_{ij} and the integration step is calculated

$$\Delta t = \frac{1}{m} \cdot \min_{i,j,\ dt>0}\left(\Delta t_{ij}\right); \ i = 1, 2, \ldots, n; \ j = i, i+1, \ldots, n, \tag{60}$$

where *m* is the integer number that determined which part of the period of the fastest particles is the time step. Thus, the choice of the integration step is, first of all, affected by motion of the fastest particles. For the problem solution not to be delayed by additional calculations, it is more reasonable to select the integration step not in each iteration, but in a certain number of them. An important issue of multilevel simulation of the problems of aerosol nanotechnologies is gradual increase of the space scale during calculation. This possibility is stipulated by the fact that during formation of nanoparticles in a gas mixture the number of atoms and molecules decreases. They combine to nanoparticles and then demonstrate a collective behavior. Thus, the number of variables of the simulation problem becomes smaller.

This process occurs at the stage of gas system simulation by the molecular dynamics method. As nanoparticles become larger, their concentration in the calculated cell under consideration decreases rapidly. Then the gas phase is no longer the source of nanoparticles and nanoparticles enlarge only due to sticking of smaller nanoparticles. Therefore, from now on it is not expedient to calculate the nanosystem by the molecular dynamics method, it is necessary to use methods of mesodynamics. Further enlargement of nanoparticles can lead to the situation when particles within the calculated cell virtually do not interact and their trajectories do not intersect. However, if we take into account the effect of nanoparticles from neighboring cells, the condensation process will continue. Thus, adequate investigation of the condensation problem of nanoparticles requires timely increase of the space scale of the cell by uniting several calculated cells into one. Since the problem is solved using the periodic boundary conditions, the space scale can be increased by symmetric mapping of atoms, molecules, and nanoparticles on the neighboring calculated cells. This problem was considered in detail in [19].

2.4. The software package

In conclusion we consider the common algorithm of simulation of the problems of aerosol nanotechnologies and indicate in which way the solutions at different structural levels agree. The methods of solution of aerosol nanotechnologies presented above allow simulation of the proceses of formation and motion of n anoparticles in different space and time scales. Each method makes it possible to simulated the system at different structural levels and demonstrates an increase of computational capacities when mathematical description of the nanosystem changes. The general scheme of calculation by different methods is presented in Figure 12.

Quantum-chemical methods of simulation allow construction of the wave function Ψ. This function is used for calculation of the structure and dimensions of molecules entering into the gas mixture. Molecular dynamics, using this information, makes it possible to calculate velocities and coordinates of atoms (both free and joined into molecules) $\bar{V}_i$, $\bar{x}_i$, and variation of these quantities with time. The result of calculation is the shape and structure of nanoparticles formed by molecules and atoms and the forces of interaction between the atoms. Simulation by the mesodynamics methods on the basis of the calculated data by the molecular dynamics method allows one to calculated linear and angular velocities of motion of nanoparticles, coordinates of the center of masses of nanoparticles $\bar{V}_i$, Θ_3^k, $\bar{x}_i$, and variation of these parameters with time. The shape and spatial structure of nanostructures formed from nanoparticles is calculated based on these data.
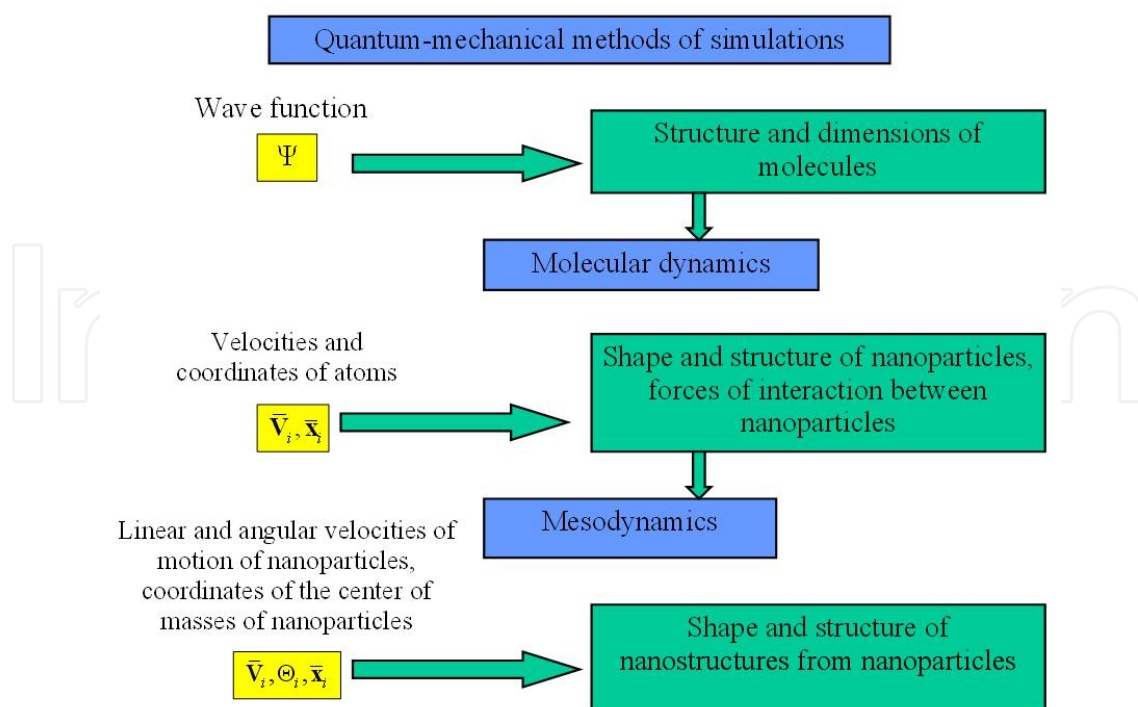
Figure 12. General scheme of the solution of problems of aerosol nanotechnologies.

It should be noted that the presented methods of calculation are not isolated from each other. In solving a number of problems they may be used simultaneously. For example, the trajectories of motion of atoms and molecules can be calculated by the molecular dynamics methods and the forces of interaction between the atoms and molecules at each calculated time step by the methods of quantum mechanics. Motion of nanoparticles in the gas phase can be treated as motion of supermolecules the trajectory of which is calculated by the mesodynamics methods and the motion of atoms and molecules of the gas mixture is calculated by the molecular dynamics methods.

The software package was created for the calculation of the above methodology (Figure 13), designed for the study of the formation of heterogeneous nanoparticles. The software package allows to multi-level mathematical simulation of the formation of nanoparticles. It consists of the initial data preparation section, the computational unit, data analysis and visualization unit and the section of data reconciliation. The initial data preparation section determines the initial conditions for simulation and generates input files for the computer unit. Computing init includes sections for quantum-mechanical calculations, molecular dynamics simulation program, and calculate the motion of nanoparticles mesodynamics methods. The simulation analysis of the system is performed in the unit of analysis and visualization. The unit solves the problem of analyzing the structure, properties and characteristics of the formed nanochatits, as well as visualization of the results. This unit supports the output files for quantum mechanics calculations, molecular dynamics and mezodinamike, and is able to reproduce both static and dynamic state of the system being modeled. Algorithms constitute unit structure, such as the establishment of the atoms are grouped in the nanoparticles, the definition of uniform composition formed from a mixture of atoms, molecules and nanoparticles, and nanoparticle properties: radius, shape, volume, bulk quantities of the
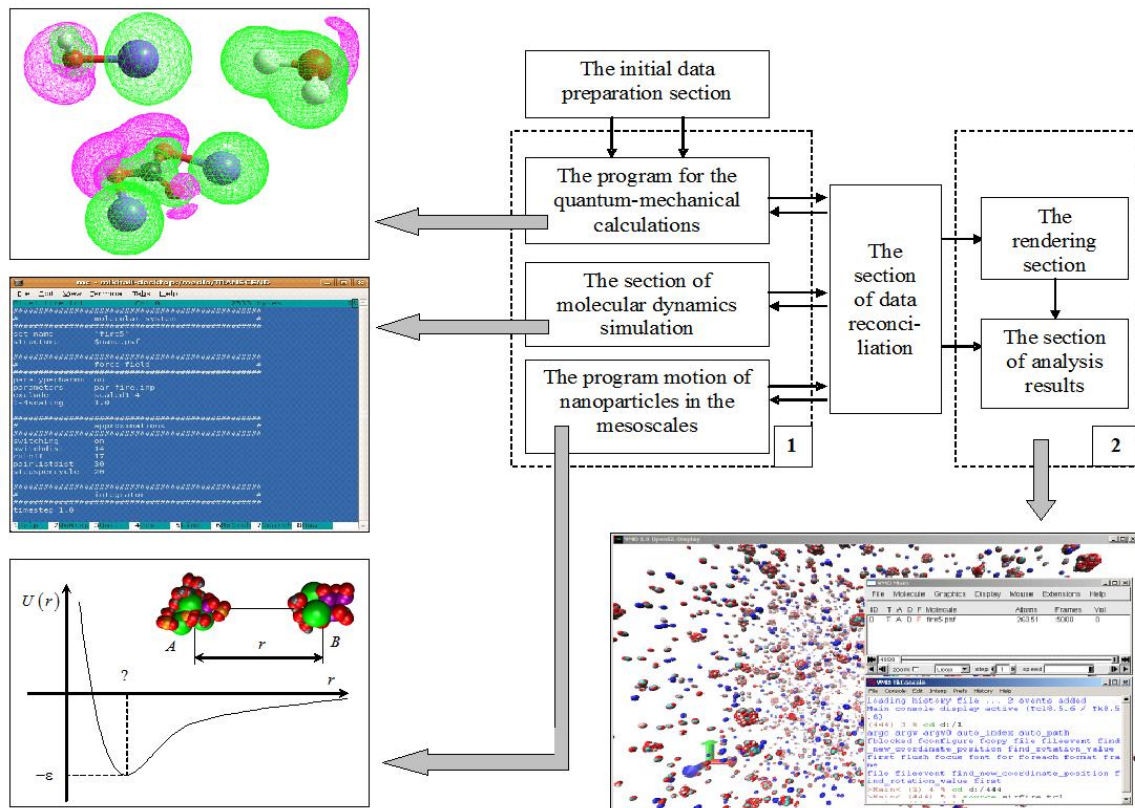
Figure 13. The structure of the software system, where 1 – compute unit 2 – unit of analysis and visualization.

surface. In addition, this module allows to determine the chemical composition and ratios of the source of the chemical elements contained in the nanoparticles, to calculate the fraction of atoms and molecules condensed into nanoparticles, to build the internal structure of nanoparticles. A detailed description of the software system is presented in the paper [20].

2.5. Technique of experimental research

Experimental investigations were carried out on two main areas:

- The study of the formation of nanoparticles in the gas phase.
- Investigation of the effect of the gas phase with nanoparticles on plants.

The experimental investigations were carried out according to the following technique.

1. The laboratory glass was prepared: it was washed, dried and degreased.
2. The glass was fixed on a holder at the distance of 150 mm from a solid-fuel grain in the laboratory cabinet.
3. The grain was ignited.
4. The laboratory cabinet was sealed.
5. The sample was held in the gas atmosphere for 5 minutes.

6. The laboratory cabinet was unsealed.

7. The sample was unfixed from the holder.

8. The sample was placed in the microscope Bikmed-1.

9. With the use of the digital camera Canon Power Shot A95, the sample was photographed at different magnifications.

10. The digital information obtained was entered into the computer Samsung Q30 and processed.

11. Then the sample was placed in the atom force microscope NTEGRA Maximus.

12. The optical image of the sample surface was built up.

13. An area on the sample surface, which was free from microparticles, was selected.

14. The above area was scanned.

15. The information in the digital form was entered into the computer and processed.

3. Results of simulation and experimental research

3.1. The analysis of the calculation results

Modelling is carried out in three steps (Figure 14). At the first step, the structures and shapes of the initial molecules are calculated using the method of quantum mechanics. In this case, the basic data are the chemical formula of the molecule, the number of bonds between the atoms and their lengths, the electrostatic charge of the atoms in the molecule, the angles between the bonds in the molecule (for molecules containing no less than 3 atoms) and some other information related to the spatial arrangement of the molecule atoms relative to each other. The second step of the calculation of the processes in the gas mixture is realized by the molecular dynamics method. The third step of the calculation is realized by the mesodynamics. The calculation of the structures and shapes of nanoparticles is carried out. The stability of nanoparticles and nanoparticles' systems in the process of their static or dynamic interaction is analyzed. The effect of the composition, shape and size of nanoparticles on their movement processes in gas medium (Brownian movement, agglomeration, sedimentation) is studied. The processes of spatial sedimentation of nanoparticles on plants are analyzed.
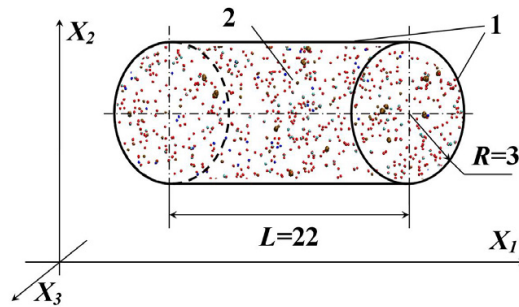
The second step of the calculation of the processes in the gas mixture is realized by the molecular dynamics method. The investigated gas mixture 1 is admitted inside a cylindrical calculation cell C_1 of length $L = 220$ nm (nanometres) and radius $R = 32$ nm. The gas mixture consists of 18 molecules of different types with a certain ratio of mass portions. For the calculations it is sufficient to take into account only six components of the gas mixture, since their mass makes 99 percent of the total mass of the system. They are the following molecules: O_2, CO_2, K_2CO_3, H_2O, N_2, MgO. The system under study contains 8850 atoms joined into 3500 molecules. The number of molecules of different types in the gas composition is determined in proportion to their mass portion in the gas mixture.

To start the calculation by the molecular dynamics method at the moment $t = 0$, we use the structures of the gas mixture molecules, which were obtained at the first step and then specify
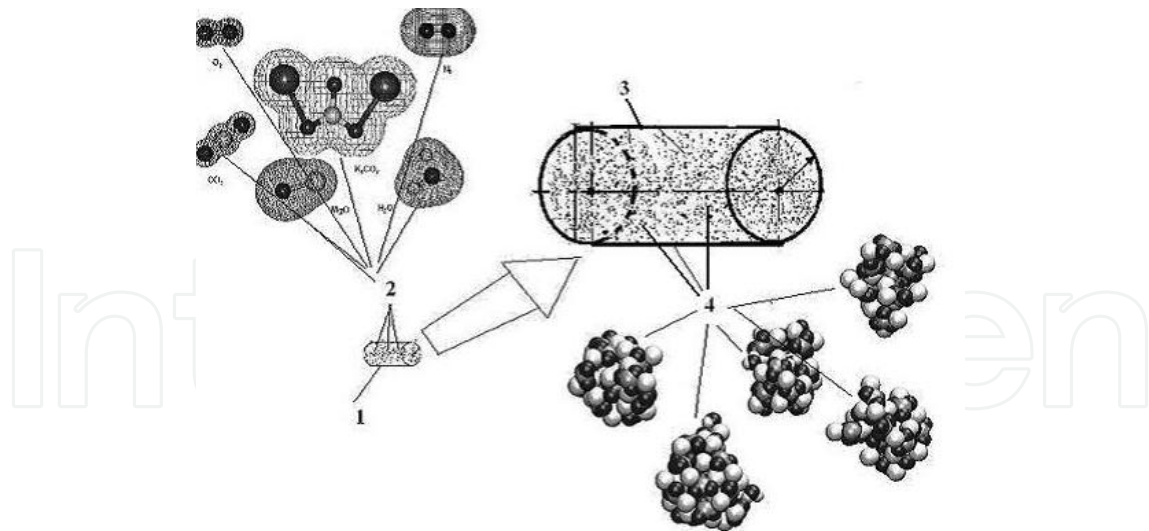
Figure 14. The settlement circuit: 1 – calculation cell C_1: 2 – molecules; 3 – calculation cell C_2; 4 – the nanoparticles.

Figure 15. The calculation scheme for modeling the process of the nanoparticle formation and movement: 1 – gas mixture containing nanoparticles; 2 – cylindrical calculation cell (the sizes are in nanometers).

Molecular formula	The number of molecules
O_2	1600
CO_2	800
H_2O	600
N_2	200
MgO	150
K_2CO_3	150

Table 1. The molecular composition of the gas mixture.

the coordinates and velocities of the atoms of all the molecules (23). The initial coordinates of the molecules $\bar{x}_{i0}$ are given based on the uniform distribution of the gas mixture molecules and their random intermixing within the calculation cell. The modules of the molecule velocities are calculated in accordance with Maxwell distribution and at an initial temperature $T_0 = 600K$. The initial temperature and the initial velocities of the molecules are determined by the relation (24).

For the velocity vector, Maxwell distribution is the product of the distributions for each of the three directions (25)–(26). Then the gas mixture is gradually cooled down to the temperature
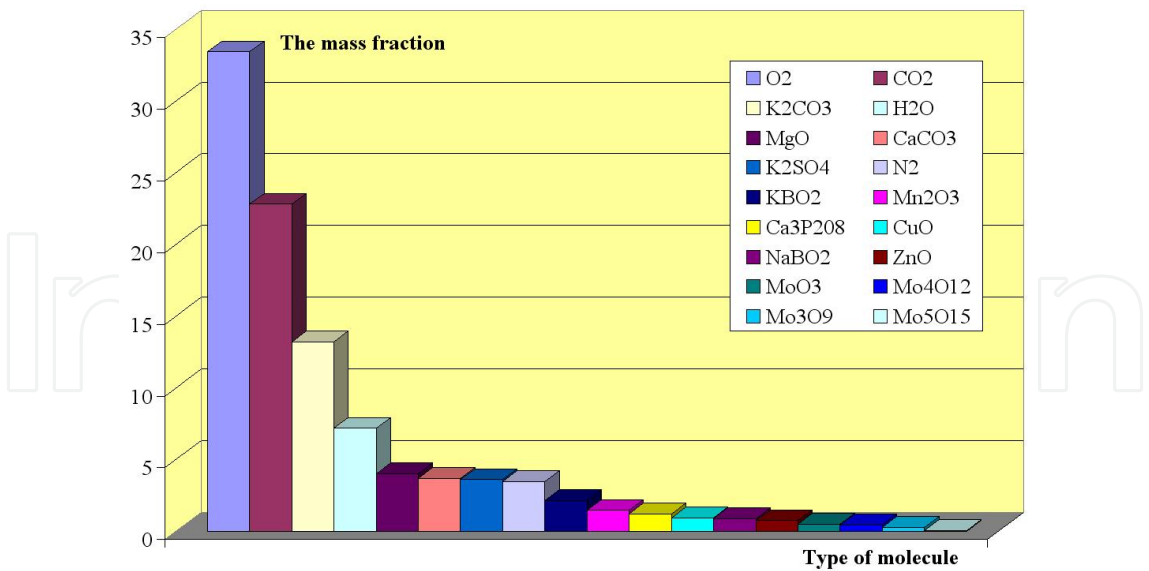
**Figure 16.** Mass portions of the molecules of the calculated gas mixture.

$T_p = 300K$ for 1.1 ns (nanosecond). The system temperature is further kept constant at the above level. The calculations are carried out based on Verlet scheme, with a step of integration with respect to the time 10^{-15} s. Thus, the period of 1 ns is calculated over one million steps of integration with respect to the time, which is quite sufficient for a detailed calculation of the main parameters of the molecular dynamic processes in the calculated gas mixture. For the interaction of the molecules with each other, the main types of forces between atoms and molecules are taken into account.

The calculation shows that nanoparticles form in the gas mixture at cooling. The analysis of the qualitative composition of the condensed nanoparticles shows that their main component is potassium. As it follows from Figure 17, the main mass of potassium (95%) transits in the condensed phase and only 5% of this element remains in gas phase.
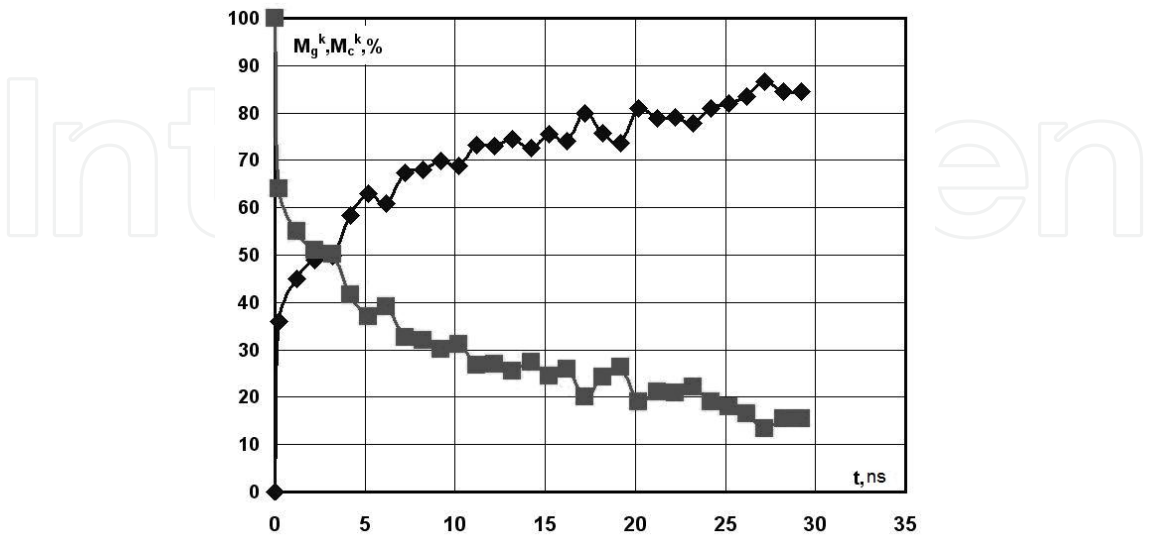
Figure 17. The variation of the condensed potassium mass and the mass of potassium in the gas phase.

Figure 18 shows the variation of volumetric density of the nanoparticles in unit of volume $Nr = N^{np}/\Omega$ with time, which form during the cooling process of the initial gas mixture. From the plot, one can see that at the initial period (about 3 ns), an intensive formation of nanoparticle takes place in the gas mixture. Their maximal density of the nanoparticles observed at $t = 4.3$ ns. It is necessary to note that during this period a noticeable variation of the number of nanoparticles is taking place. This is indicative of the presence of simultaneous and competing processes of the formation and decomposition of nanoparticles. By the 55th nanosecond, these processes subside; new particles do not form, and previously formed nanoparticles consolidate. Therefore, the density of the nanoparticles gradually reduces to $10^{22,5}$ with time. However, despite the decrease in the quantity of the nanoparticles, their total volume Ω_S is increasing with the time (Figure 19). From this figure, it follows that the volume of the nanoparticles is actively increasing during the initial period, and then the rate of the nanoparticle volume growth is decreasing. This also indicates that the formation of new nanoparticles is subsiding. By the 75th nanosecond, the nanoparticle volume growth practically stops.
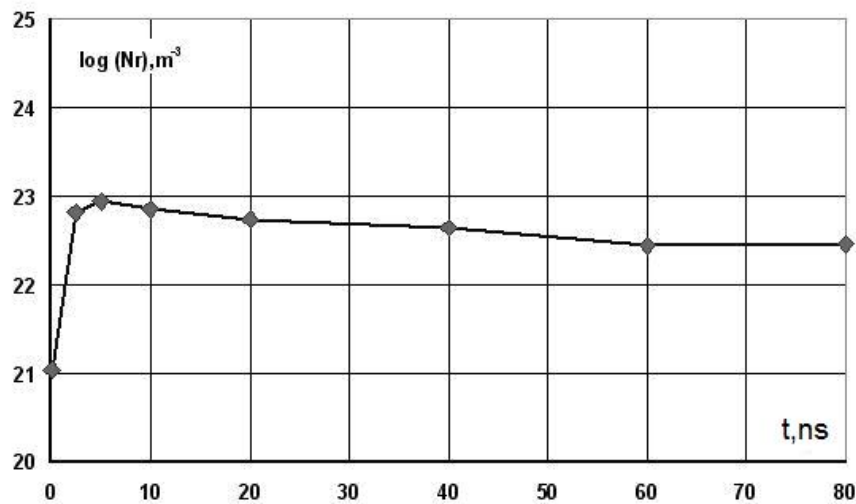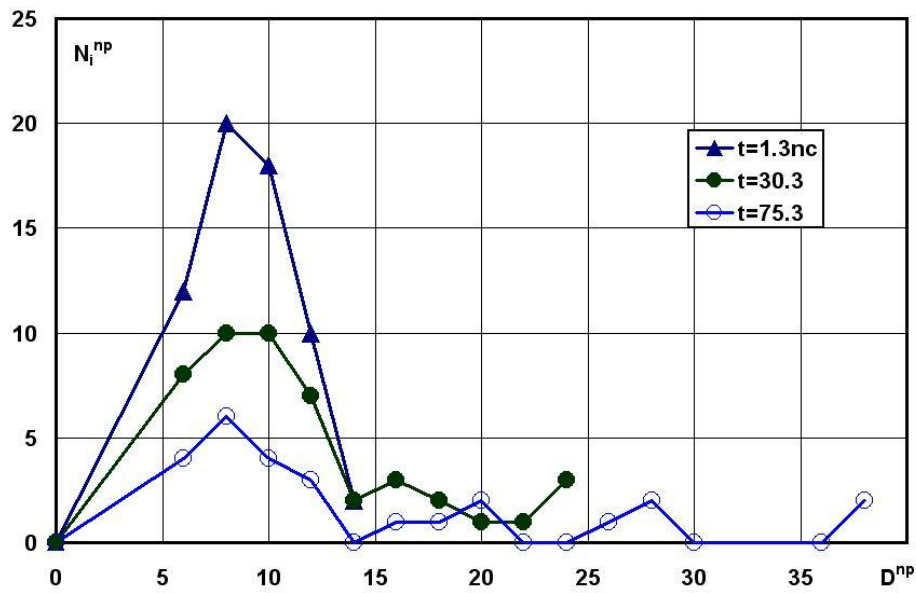

Figure 18. The variation of the number of nanoparticles in the unit of volume with time.

Similar dependences are observed when the mass components of the system calculated are considered. The content of the gas phase is decreasing, and the content of the condensed phase is increasing; further the ratio of the phases remains constant. Hence, only about 15% of the system substance turns into condensate and 85% remains in the gas phase. Then the gas phase is not the nanoparticle source any more and the nanoparticle enlargement takes place solely due to the reason that small nanoparticles stick together. From this moment, therefore, it is expedient to calculate a nanosystem with the use of the mesodynamics methods rather than the molecular dynamics method. This is the last stage of the simulation.

The presence of the nanoparticle consolidating process is confirmed by an increase in the number of coarse nanoparticles with time. Figure 20 shows histograms of the distribution of the nanoparticles by sizes at different moments: $t = 1.3; 30.3; 75.3$ ns. The maximum of this distribution does not practically shift with time relatively to the size of the nanoparticles; with a decrease in the number of the nanoparticles, the quantity of the coarser nanoparticles is growing.
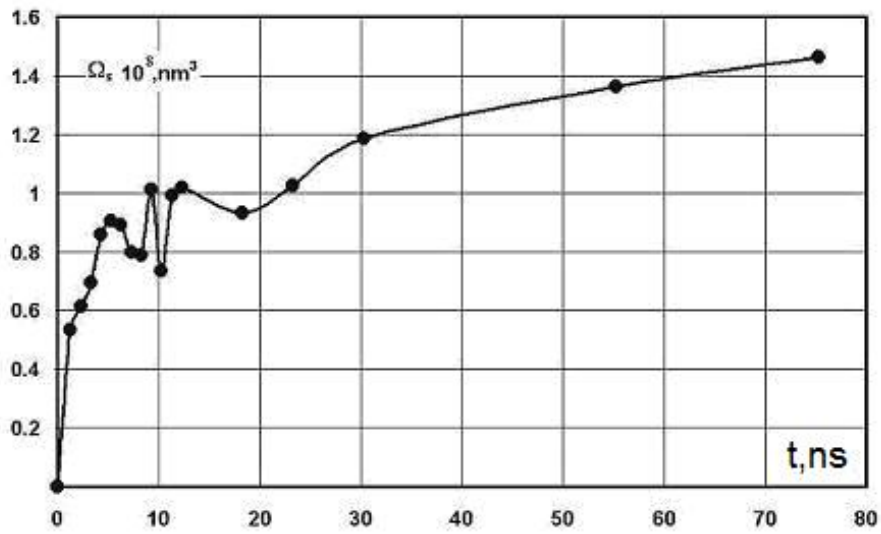
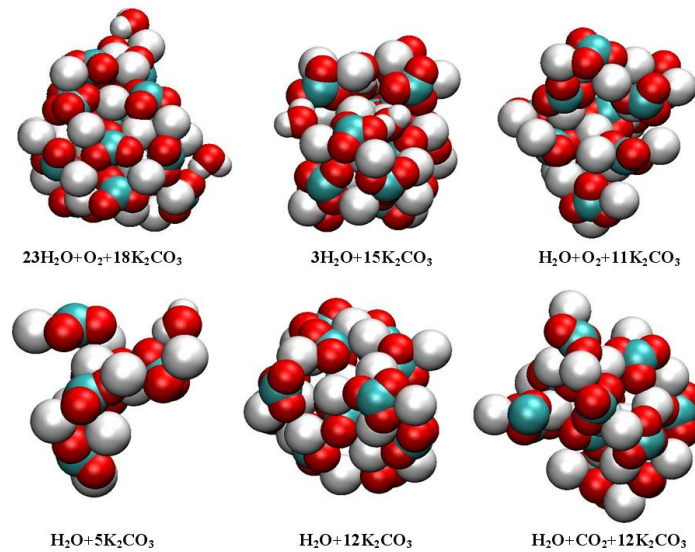**Figure 19.** The variation of the total nanoparticle volume Ω_S with time.

Figure 20. The variation of the distribution of nanoparticles by sizes with time.

For the simulation, a calculation cell C_2 is used (Figure 14-3), and the nanoparticle movement (Figure 14-4) is calculated without taking into consideration the movement of the gas phase molecules. The calculation cell C_2 is five times larger than a cell C_1. Consequently, the volume of the calculation cell C_2 is 125 times larger than the volume of the cell C_1 and, hence, the number of particles in it is 125 times larger than that in the cell C_1. For this calculation stage, the initial conditions are determined in accordance with the relations

$$t_2^0 = t_1^*, \, \bar{\mathbf{X}}_i \subset \Omega_2, \, \bar{\mathbf{V}}_\mathbf{i} = \frac{1}{M_i} \sum_{j=1}^{N_i} m_j \bar{\mathbf{V}}_j, \tag{61}$$

where $\bar{\mathbf{X}}_i$ are coordinates of the nanoparticle centre of mass; m_j and $\bar{\mathbf{V}}_j$ are masses and velocities of atoms contained in a nanoparticle, respectively; M_i and m_j and $\bar{\mathbf{V}}_i$ are masses of nanoparticles and velocities of the nanoparticles' centres of mass, respectively; t_1^* and t_2^0 are the time of the completion of the second stage and the time of the beginning of the third stage of the calculations, respectively. The mesodynamics calculations show that with time nanoparticles combine into larger ones. Their number decreases down to 16, and their average size increases fivefold approximately. This allows a sevenfold increase of the calculation cell. In this case, in comparison with the calculation cell C_2, its volume increases by 343 times and the number of nanoparticles in it reaches 5488. The step of integration with respect to the time is 10^{-13} s.

Thus, in the example considered, the use of the mesodynamics method allowed increasing the calculation cell volume and the volume of the modelled space by 42875 times. The integration step increased hundredfold, and at the same time, the number of the variables remains almost unchanged. The structures and compositions of the formed nanoparticles are shown in Figure 21. The calculations show that the nanoparticles mainly consist of the K_2CO_3 molecules with small inclusions of the molecules of water, carbon dioxide and oxygen.

$23H_2O+O_2+18K_2CO_3$ $3H_2O+15K_2CO_3$ $H_2O+O_2+11K_2CO_3$

$H_2O+5K_2CO_3$ $H_2O+12K_2CO_3$ $H_2O+CO_2+12K_2CO_3$

Figure 21. The structures and compositions of the nanoparticles.

The investigation of the movement of nanoparticles is important since it determines the character of the interaction of the nanoparticles and the surface. Below, the calculated movement paths for a massive nanoparticle (Figure 22-a) and a particle of a smaller size (Figure 22-b) are given.

From the figures, it is clear that the nanoparticles are moving in a random and complex way. Moreover, a massive nanoparticle passes a shorter path than a particle with a smaller mass. Its path is "smoother". Judging by the shapes of the paths, one can assume that the particles are in Brownian motion, moving in different directions in space. Consequently, it can be suggested that the process of their sedimentation occurs on the surfaces that are randomly oriented in space, in other words, on all the surfaces of a plant.
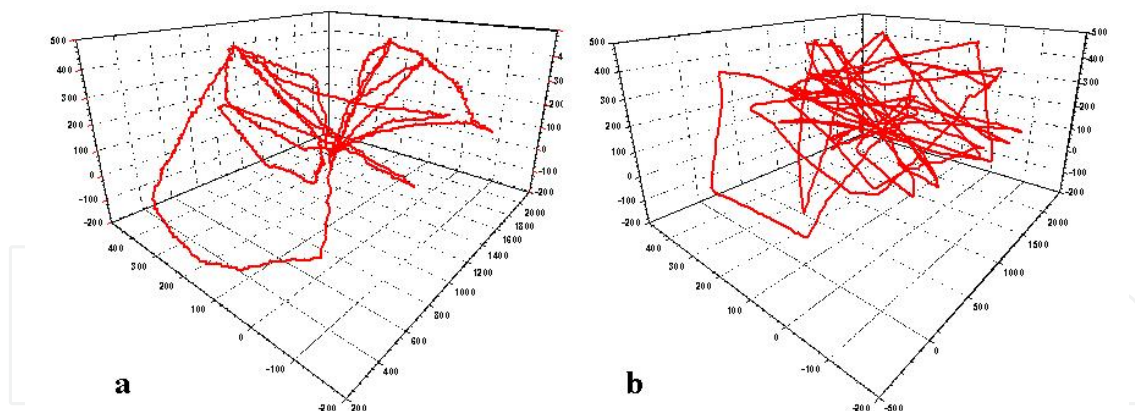
Figure 22. Brownian motion path of a massive nanoparticle (a) and Brownian motion path of a nanoparticle with a smaller mass (b).

3.2. The analysis of the experimental results of nanoparticle formation

The maximal size of the optically-investigated sample area was 7125x5400 μm and the minimal size was 95x72 μm. The accuracy of the determination of the microparticle boundary was 0.2 μm in this case. The size of the area scanned with the use of the power atomic microscope was 1.5x1.5 μm. The accuracy of the determination of the nanoparticle boundary was 2 nm.
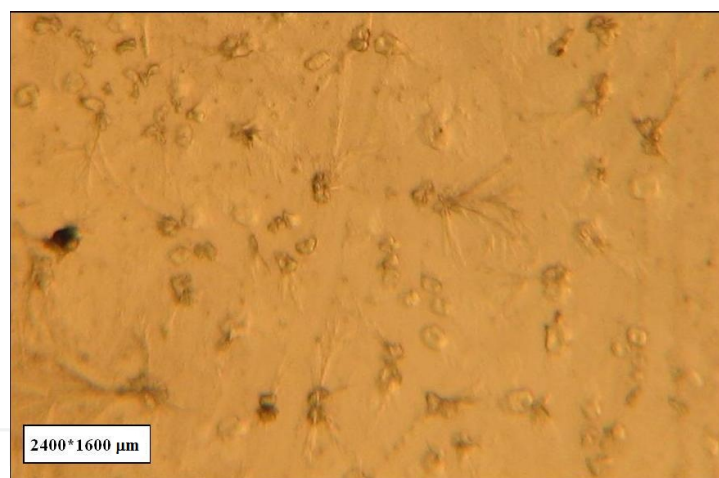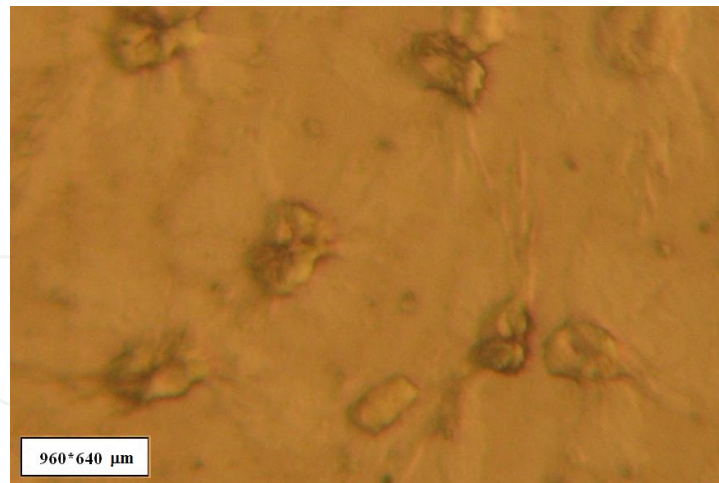

Figure 23. Optical image of particles deposited on the glass (75x magnification).

Let consider the experimental investigation results on the forms and distribution of the sizes of particles deposited on a glass surface from the gas phase. The investigations conducted show that the sizes of the particles deposited on the glass in accordance with the above technique lie in a wide range: from tens of microns to tens of nanometers. In Figure 23, a 75x enlarged view of the sample is presented. It is seen from the figure that there are particles of 100 μm in size on the glass. However, the smaller particles are seen as well. A more enlarged image presented in Figure 24 (187.5x magnification) allows a reliable identification of a particle with the size of about 10 μm.
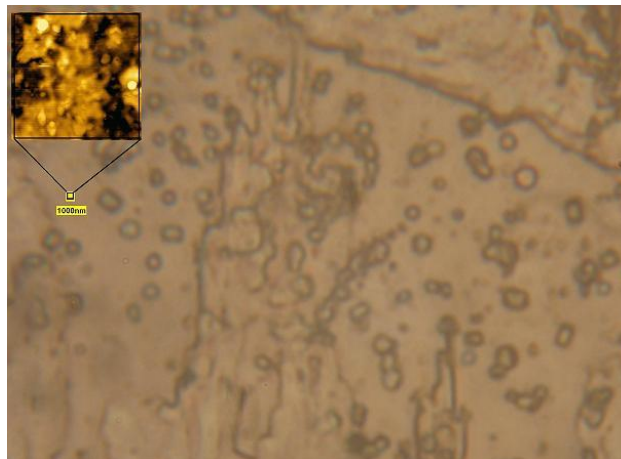
In Figure 25 an optical-digital image of the particles deposited on the glass (5375x magnification) shows that the particles with smaller sizes (1 micron and less than 1 micron)
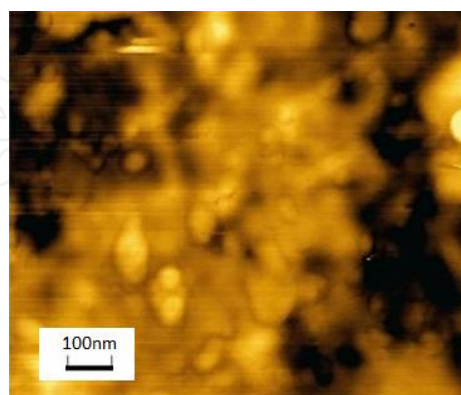
Figure 24. Optical image of particles deposited on the glass (185.5x magnification).

are also observed. It should be noted that further digital magnification leads to a no distinct image and does not allow establishing the sizes of particles reliably.

Figure 25. Optical-digital image of particles (5375x magnification, image size: 95 μm x 72 μm).

Figure 26. Image of nanoparticles deposited on the glass, which was obtained using the power atomic microscope (image size: 1000 nm x 1000 nm).

In Figure 25, one also can see an area of 1000 nm (1 μm) that was investigated with the use of the atomic-force microscope. The pattern of scanning is presented on an enlarged scale in

The fruits of the plant	The control plants	Plants treated with aerosol
Cucumbers	1.00	1.80
Beet	3.07	3.45
Radish	0.73	2.10

Table 2. The content of potassium in vegetables in milligrams.

Figure 26. The pattern of scanning shows that nanoparticles have precipitated on the glass. The size distribution histogram for nanoparticles is displayed in Figure 27. It follows from the plot that most nanoparticles lie in the range from 15 nm to 45 nm.
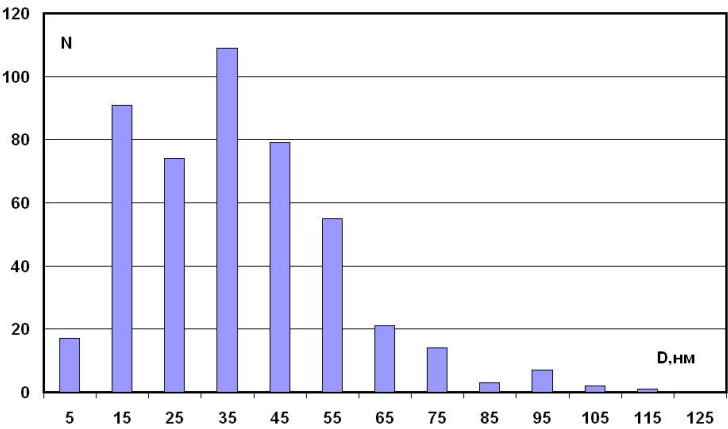
Figure 27. Size distribution histogram for nanoparticles.

3.3. Research of influence of the gas phase with nanoparticles on plants

Experimental researches included: structural botany researches, studying of activity of the photosynthetic processes, the biochemical analysis of ferment activity. Also studying of nanoaerosol action on regulation of a potato growth and dynamics of growth and development of salad cultures were carried out.

Let's compare amount of mineral fertilizers traditionally used at cultivation of plants in hothouses with amount of fertilizers at aerosol nutrition of plants. In the closed soil need of plants for nitric fertilizers (urea, ammoniac saltpeter) is 1.1 kg/m^2, and need for potash fertilizers is 1.4 of kg/m^2 [21]. As mineral fertilizers are brought in the form of water solution with concentration from 0.5% to 0.8%, the total amount of solution brought in the soil is 80 80 liters per m^2. The amount of mineral fertilizers thus is 6.97 kg/m^2. Processing by means of nanoaerosols is carried out one time in 5–7 days. For all period of growth of plants the fertilizer expense is only 8–14 g/m^2. On the average, it approximately in 500 times is lower than amount of the mineral fertilizers brought in the traditional way in the soil. Respectively and harmful substances it is brought less. First of all change of the maintenance of various elements (bohrium, manganese, zinc, cobalt, magnesium, potassium, calcium and iron) in samples of plants after processing by an aerosol was investigated. Experiments confirmed increase of the maintenance of elements of a nutripion in various parts of plants (Table 2–3).

Let's consider the results of studies on the effects of nanoparticles regenerants of potato. The work was carried out jointly with the Institute of Experimental Botany, National Academy of

Plant	Number of samples	Type of treatment	The content of elements, %				
			B	Cu	Mn	Mo	K
Tomatoes	1	Control	37.5	12.4	43.2	0.8	6.8
		Aerosol	74.0	43.0	60.0	11.9	7.5
	2	Control	33.3	11.5	35.5	0.6	8.8
		Aerosol	72.6	50.8	45.9	11.9	7.5
Cucumbers	1	Control	45.0	9.3	17.5	4.7	5.2
		Aerosol	67.2	29.1	14.3	14.0	4.0
	2	Control	30.0	8.3	15.9	0.8	3.2
		Aerosol	70.5	24.0	27.0	4.3	3.8

**Table 3.** The content of elements in the leaves of plants.

Belarus. The dynamics of growth in regenerants of potato micropropagation in the prolonged culture of morphometric characteristics was considered. Before each aerosol treatment were measured morphometric parameters and monitoring of rooting cuttings explants. The data showing a clear lead in the growth processes of regenerants of potato varieties Dolphin processed aerosol to 12 days of observation was obtained (Figure 28).
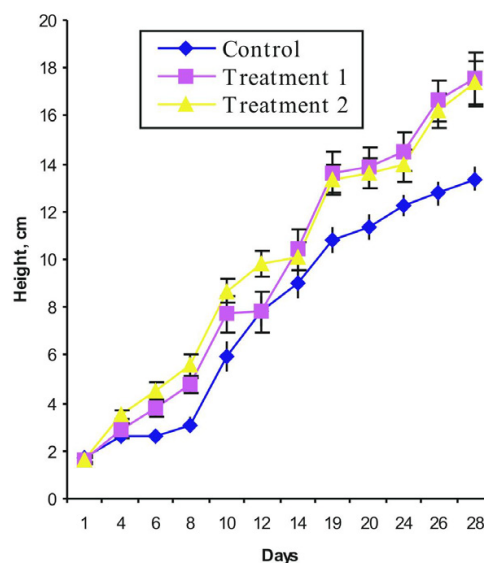
Figure 28. Growth dynamics of potato varieties Dolphin from the experimental data.

As can be seen from Figure 29 experimental plants are actively developing, exceeding the height of control plants at 1.22 and 1.19 times (treatment 1 and 2, respectively). A similar plant development was supported by Figure 29, which displays the daily activity of the growth of plants as they develop.

For plants, left for further growth and development in plastic containers, we observed for 42 days. In Table 4 was shown that lead to the growth of experimental plants and stored at the age of 42 days: plants with processing options 1 and 2 at 1.45 and 1.44 times higher than controls at the same height on the formation of leaves and internodes.
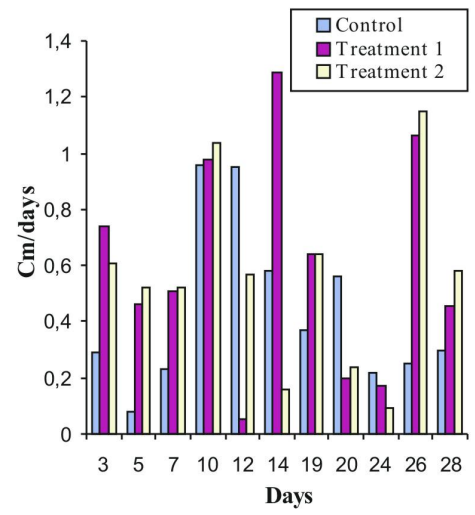
Figure 29. The growth rate of potato varieties Dolphin for the period of observation from the experimental data.
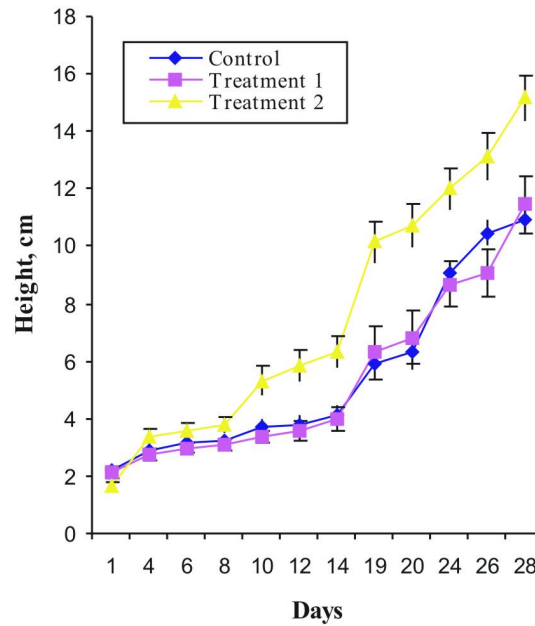
Version	Height, cm	Number of leaves, items	Number of internodes, items	Wet weight, g		
				leaves	stems	roots
Control	22.47±1.04	11.06±0.66	15.75±0.75	2.69±0.50	1.77±0.22	0.47±0.13
Treatment 1	32.69±1.45	10.87±0.59	16.12±0.39	2.78±0.51	2.76±0.37	0.94±0.23
Treatment 2	32.44±4.43	11.44±0.76	16.69±0.81	2.68±0.53	2.59±0.32	0.72±0.14

Table 4. Morphological characteristics of potato cultivar Dolphin at harvest at age 42 days.

The development of potato varieties Lazurit is slightly different from class Dolphin on the dynamics of growth. As follows from Figure 30 plants in a series of treatment 2 exceed the height of the control and experimental plants (treatment 1) to 28 days by 38% and 32% respectively. The plants left in the plastic containers for further growth and development, as well as in the case of grade Dolphin, were conducted further follow-up.

As shown in Table 5 advantage of the growth experienced in the plant varieties Lazurit age of 42 days over the control is saved. Plants with treatment 1 and 2 were of 1.87 and 1.96 times higher than the control plants in height and 1.13 and 1.17 times the number of internodes. The mass of the leaves advantage of control plants, with an equal number of it's with the experimental data shows about the formation of a dense leaf. At a height equal to the control plants and the option of processing 1 plants have experienced a significant differences in the accumulation of fresh weight of leaves and roots of 2.2 and 3.4 times. At the age of 42 days in 40% of plant varieties Lazurit (treatment 2) were formed side shoots on the average length of 4.5 cm. In control plants and the processing 1plants the side shoots are not detected. We can assume that a often treatment of options 1 and 2 (one day) was contributed to the formation of young growing aerial parts of plants, thus extending the growing season.

Results of studies of dry matter content in some parts of potato plants Lazurit (Table 6) showed that frequent drug treatment "Greenhouse" leads to a "rejuvenation" of plants, reducing the synthesis of organic matter, such as starch.

Figure 30. Growth dynamics of potato varieties Lazurit for different conditions experience.

Version	Height, cm	Number of leaves, items	Number of internodes, items	Wet weight, g		
				leaves	stems	roots
Control	18.17±2.17	10.83±1.18	11.83±0.60	4.93±0.78	2.48±0.20	1.15±0.16
Treatment 1	34.03±1.25	9.00±0.59	13.37±0.56	2.21±0.50	2.53±0.34	0.34±0.09
Treatment 2	35.63±1.01	10.87±0.54	13.80±0.39	3.15±0.70	3.11±0.70	1.01±0.29

Table 5. Morphological characteristics of potato varieties Lazurit at the age of 42 days.

| Version	Part of absolutely dry mass, %			The absolutely dry mass, g		
	leaves	stems	roots	leaves	stems	roots
Control	22.47±1.04	11.06±0.66	15.75±0.75	2.69±0.50	1.77±0.22	0.47±0.13
Treatment 1	32.69±1.45	10.87±0.59	16.12±0.39	2.78±0.51	2.76±0.37	0.94±0.23
Treatment 2	32.44±4.43	11.44±0.76	16.69±0.81	2.68±0.53	2.59±0.32	0.72±0.14

Table 6. Characterization of potato varieties Lazurit at the age of 42 days.

Consider the results of a study of the photosynthetic activity of the processes of photosynthesis. About the functioning of the photosynthetic transport chain in plants can talk on the basis of photoinduced changes in absorption or fluorescence. As is known, light green plants is accompanied by increased fluorescence yield. Fluorescence undergoes complex transient phenomena before reaching a constant level. It is assumed that the induction of fluorescence due to the variable part of fluorescence of chlorophyll a, the output of which depends on the state of the active center of photosystem and the rate of electron transfer. The accurate registration of the fluorescence changes for small periods of time is required to obtain a complete picture of fluorescence induction. To characterize the photosynthetic

processes determine the rate of decay of variable chlorophyll fluorescence was used, reflecting the photochemical activity (FHA).

The systematic study of the change dynamics in the decay rate of variable fluorescence of chlorophyll per day processing plants nanoaerosol was carried out (after 2, 4, and 6 hours after treatment). Analyzing the results, you may notice that the substance treatment of "Greenhouse" vegetative regenerants causes changes in the studied parameters as the Dolphin class and a grade Lasurit. Changes in the direction of activation of photosynthetic activity strongly manifested at the Dolphin class. The second version of the experience with pre-treatment plants before meristem cuttings was more sensitive to changes in photosynthetic activity of plants. The additional introduction of CO_2 in the nanoaerosol processing, gives rise to a new round of metabolic processes, especially evident after 16–19 treatments when the plants are in the process of budding and early flowering. The relative values of the parameter Ft/Fm, reflecting the velocity of the electron transport chain of chloroplast membranes is in the range 0.3–0.4, which corresponds to the high photosynthetic activity. In the leaf tissue homogenates regenerantnyh plants varieties Lasurit and Dolphin processed aerosol "Greenhouse", and in the control group the content of peroxidase have been studied, which is an indicator of physiological stress of plants. With an increase in enzyme activity can be stated that the action of a factor caused a chain of physiological and biochemical processes that lead to the response to stress.

Such a reaction may have immune activating effect. As a result of the immune enzyme analysis with antibodies to the enzyme peroxidase, it was found that the drug "Greenhouse" causes a change in the activity of this enzyme. Moreover, there are reliable changes in activity (significance level 0.01), depending on the multiplicity of processing. The results of determination of peroxidase activity are shown in Figure 31.
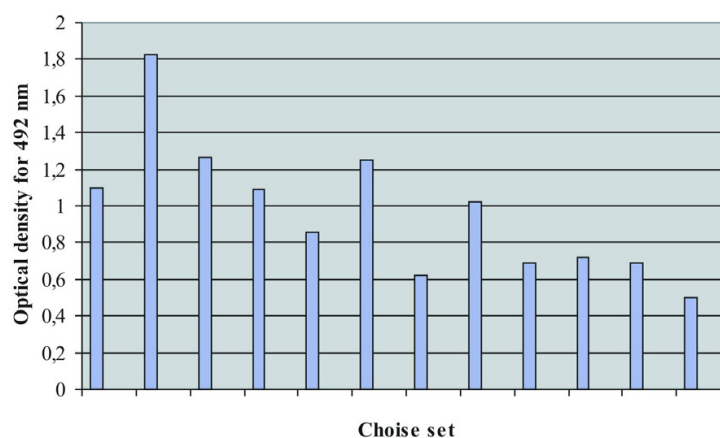

Figure 31. Peroxidase activity in membrane fractions of regenerated potato varieties Dolphin and Lazurit.

As a result of the experiments, significant differences in the value of this indicator depending on the variety were observed. In the variety Dolphin pretreatment before the cuttings a similar reaction regenerates the stress was caused that was manifested in an increase in peroxidase activity. In the grade Lazurit option 3, on the contrary, was the stress is not sensitive (Table 7).

#	Version	Treatment 1	Treatment 2	Treatment 3	Treatment 4	Treatment 5
Grade Dolphin – medium early					
1	Control	0.776	0.806	0.854	0.760	0.836
2	Variant 2	0.846	0.906	0.917	0.940	0.909
3	Variant 3	1.351	1.390	1.441	1.387	1.366
Grade Lazurit – early					
4	Control	1.358	1.433	1.488	1.505	1.554
5	Variant 2	1.981	2.031	2.097	2.121	2.073
6	Variant 3	0.949	0.979	1.003	0.996	0.979

Table 7. Change in optical density at $\lambda = 492$ under the action of peroxidase enzyme spray "Greenhouse" in regenerant leaves of potato varieties Dolphin and Lazurit.

We studied the effects on the biological properties of nanoaerosol seeds: vegetables – carrots, beets, kale, forage grasses – goat grass, clover, plants in greenhouses: cucumber, sweet pepper, tomato, parsley, lettuce. Work was carried out with seeds of varying quality. Germination of control samples in different batches ranged from 27% to 99%. Some of the seeds before the experiments were struck by bacterial diseases. The results of the studies have shown high efficiency of this method of improving the biological properties of the seeds. In all cultures were obtained by increasing the energy of germination up to 18% and 20% germination. For control group of seed germination was 67% and 71% germination, and in an experimental batch exposed to a special gas environment, these figures were 87% and 93%, respectively. The study of the nanoaerosol treatment on growth and development of salads also confirmed the high efficiency of the proposed technology. Comparison of germination of lettuce seeds "Gribovsky curly" grade is shown in Figure 32.
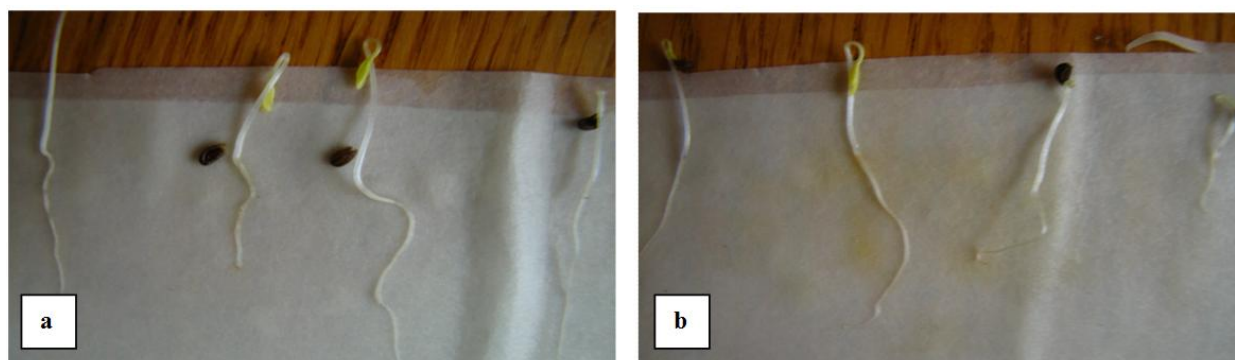
Figure 32. Germination of lettuce seeds "Gribovsky curly" grade (treatment of "Greenhouse" - a, control - b).

It is evident that the seeds after nanoaerosol treatment developed intensively. In addition – treated seeds during storage, preparation for the planting and growing season were significantly more resistant to various fungal diseases. Observations over three years for the treated seeds showed that the rate of germination and vigor are in time at a high level. Reducing of germination does not exceed 1–1.5% per year. Pilot studies according to productivity of potatoes, carrots, a tomato and cucumbers showed that the crop increases on the average by 20–30% [5].

4. Conclusion

1. In the present paper, the multilevel mathematical model is developed for solving the problem of formation, movement, hashing, and condensation of nanoparticles by methods of quantum mechanics, molecular dynamics and mesodynamics, describing the behavior of nanoaerosols for studying the processes of condensation of nanoaerosols for the nutrition of plants.

2. The numerical calculations have showed:
   - the growth of nanoparticles and their interactions depend on time and on the number of free molecules that actively form nanoparticles;
   - the speed of association of molecules into nanoparticles depends on temperature and pressure and molecules concentration in the gas medium;
   - the molecules of potassium carbonate and water are into nanoparticles and therefore they can be used for the nutrition of plants.

3. Experiments have confirmed that in aerosols nanoparticles are formed.

4. In experimental studies influence nano- and the microparticles generated by specially solid propellant composition, on biological objects (plants, fruits and seeds) is established. A number of positive effects which are widely used already today hothouse and the farms working with plants in hothouses were received.
   - Productivity increase to 30%, increase in ovaries of fruits, development of more powerful stalk and leaves and uniformity of maturing of fruits was established.
   - Plants become more resistant to diseases.
   - Early fructification and increase in term of vegetation is observed.
   - Germination of various plants seeds increases to 100%.
   - From treated seeds produced high-quality embryos, superior on all counts of untreated seed embryos.
   - Stability of sprouts to fungous diseases raised.

5. Method of foliar spray fertilizer plant almost does not require any material costs and specialized equipment. This method significantly reduced the complexity of foliar feedings. On average, holding a spray fertilizer on the area of 1000 m^2 spent 0.3 person/hour, and overall costs are reduced by 40% in recalculation per m^2, while increasing the productivity of more than 20%.

6. Technology makes it possible to make fertilizer to the requirements of the manufacturer, to add or to remove from it those nutrients that are necessary to use soil or certain climatic regions.

7. The executed theoretical and experimental studies allowed use this technology for growing various vegetables and crops in greenhouses of Russia, Byelorussia, the Ukraine and China. Practical value of the received results is very good.

Author details

Vakhrushev A.V., Fedotov A.Yu. and Vakhrushev A.A.
Institute of Mechanics, Ural Branch the Russian Academy of Sciences, Izhevsk, Russia

Golubchikov V.B and Golubchikov E.V.
Join Stocks Company Nord, Perm, Russia

5. References

[1] Alikin V.N, Vakhrouchev A.V, Golubchikov V.B, Lipanov A.M and Serebrennikov S.Y (2010) Development and Investigation of the Aerosol Nanotechnology. Moscow: Mashinostroenie. 196 p.

[2] Golubchikov V.B, Sibiriakov S.V, Levin D.G, Alikin V.N (2006) The Regulated Gas Medium for Preseeding Processing Seeds of Vegetables. Hothouses of Russia j. 1: 55.

[3] Vakhrouchev A.V, Golubchikov V.B (2006) Numerical Investigation of the Dynamics of Nanoparticle Systems in Biological Processes of Plant Nutrition. Abstracts of Conference on Nanoscience and Technology ICN&T. Basel, Switzerland: 209.

[4] Vakhrouchev A.V, Golubchikov V.B (2007) Numerical Investigation of the Dynamics of Nanoparticle Systems in Biological Processes of Plant Nutrition. Journal of Physics, Conference Series. 61: 31–35.

[5] Vakhrouchev A.V, Golubchikov V.B (2006) The Regulated Gas Medium with a Set of Nanoparticles Generated by the Solid Fuel Composition as a Method for Producing Eco-vegetables. NanoBiotech World Congress, Boston, MA, USA: 16–17.

[6] Chushak Y (2001) Molecular Dynamics Simulations of the Freezing of Gold Nanoparticles. Eur. Phys. J.D. 16: 43–46.

[7] Vakhrouchev A.V, Fedotov A.Y, Vakhrushev A.A, Golubchikov V.B, Givotkov A.V (2011) Multilevel Simulation of the Processes of Nanoaerosol Formation. Part 1. Theory Foundations. Nanomechanics Science and Technology: An International Journal. Vol. 2, issue 2: 105–132.

[8] Cagin T, Che J, Qi Y, Zhou Y, Demiralp E, Gao G, Goddard III W (1999) Computational Materials Chemistry at the Nanoscale. J. 1: 51–69.

[9] Steinhauser O.M (2008) Computational Multiscale Modelling of Fluids and Solids. Theory and Application. Berlin: Springe. 428 p.

[10] Marx D, Hutter J (2008) Ab Initio Molecular Dynamics: Basic Theory and Advanced Methods. Cambidge: University Presse. 567 p.

[11] Brooks B.R, Bruccoleri R.E, Olafson B.D, States D.J, Swaminathan S and Karplus M (1983) CHARMM: A Program for Macromolecular Energy Minimization, and Dynamics Calculations. J. Comput. Chemistry. Vol. 4, issue 2: 187–217.

[12] Gauss J (2000) Molecular Properties, Modern Methods and Algorithms of Quantum Chemistry. Proceedings, Second Editions. 3: 541–592.

[13] Heermann D.W (1986) Computer Simulation Methods in Theoretical Physics. Berlin: Springer-Verlag. 148 p.

[14] Holian B.L (2003) Formulating Mesodynamics for Polycrystalline Materials. Europhysics Letters. 64: 330–33.

[15] Vakhrushev A.V (2009) Modeling of the Nanosystems Formation by the Molecular Dynamics, Mesodynamics and Continuum Mechanics Methods. Multidiscipline Modeling in Materials and Structures. Vol. 5, issue 2: 99–118.

[16] Landau L.D, Lifshits E.M (1972) Quantum Mechanics. Moscow: Science. 368 p.

[17] Burkert U, Allinger N.L (1982) Molecular Mechanics. Washington D.C.: ACS Monograph. 339 p.

[18] Imry Y (2002) Introduction to Mesoscopic Physics. Oxford: University Press. 236 p.

[19] Vakhrushev A.V, Fedotov A.Y, Vakhrushev A.A (2011) Modeling of Processes of Composite Nanoparticle Formation by the Molecular Dynamics Technique. Part 1. Structure of Composite Nanoparticles. Nanomechanics Science and Technology: An International Journal. Vol. 2, issue 1: 9–38.

[20] Fedotov A.Y, Vakhrushev A.V (2011) The Software Package for Multi-level Modeling of the Formation of Heterogeneous Nanoparticles ComplexDyn v.5.0. Certificate of Registration of electronic resource number 17335, Russian Federation: 1–6.

[21] Golubchikov V.B, Sharupich V.P (2002) Foliar spray plants as a way of saving in greenhouses. Greenhouses of Russia. 2: 15–24.